

Hindsight Learning for MDPs with Exogenous Inputs

Sean R. Sinclair¹ Felipe Frujeri² Ching-An Cheng² Adith Swaminathan²

¹ School of Operations Research and Information Engineering, Cornell University

² Microsoft Research, Redmond

Abstract

We develop a reinforcement learning (RL) framework for applications that deal with sequential decisions and exogenous uncertainty, such as resource allocation and inventory management. In these applications, the uncertainty is only due to exogenous variables like future demands. A popular approach is to predict the exogenous variables using historical data and then plan with the predictions. However, this indirect approach requires high-fidelity modeling of the exogenous process to guarantee good downstream decision-making, which can be impractical when the exogenous process is complex. In this work we propose an alternative approach based on *hindsight learning* which sidesteps modeling the exogenous process. Our key insight is that, unlike Sim2Real RL, we can revisit past decisions in the historical data and derive counterfactual consequences for other actions in these applications. Our framework uses hindsight-optimal actions as the policy training signal and has strong theoretical guarantees on decision-making performance. We develop an algorithm using our framework to allocate compute resources for real-world Microsoft Azure workloads. The results show our approach learns better policies than domain-specific heuristics and Sim2Real RL baselines.

1 Introduction

Reinforcement learning (RL) has been successfully applied to systems applications, like inventory control [42], power grids [19], jitter buffers [31], and resource allocation [53]. Despite treating the system as a black box, RL algorithms have shown to outperform carefully tuned heuristics designed by domain experts [25]. However, existing RL successes rely heavily on access to large and diverse logged data as well as computational resources that is significantly larger than that used by domain heuristics [54]. These prerequisites make current RL techniques infeasible in resource constrained applications. It is therefore desirable to have more structured RL algorithms that can exploit domain knowledge to perform more efficient policy search.

One promising structure we can leverage for designing more efficient RL algorithms is the probabilistic independence property in the decision making process. In many of the above applications, the system is only partially unknown and the only uncertainty is due to *exogenous* variables, like resource demands or future weather, that are *independent* of the agent’s decisions. Consider virtual machine allocation in the cloud as an example [41]. Given a trace of exogenous inputs (i.e. the sequence of virtual machine requests) we can simulate the actions and rewards obtained by *any* policy, since the dynamics follow a known rule to update the available capacity on the assigned physical hardware, and the rewards (e.g., wasted capacity) are completely determined by the current state of the system. Credit assignment with known independence is simpler, leading to opportunities for new efficient RL algorithms.

Contact Author: Sean R. Sinclair (srs429@cornell.edu)

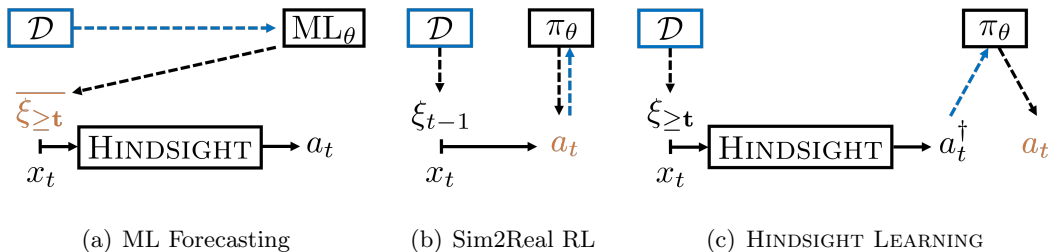


Figure 1: Two existing approaches to solve MDPs with exogenous inputs and our HINDSIGHT LEARNING framework. Dashed lines indicate data-driven or ML-driven inputs, solid lines indicate transitions using prior knowledge, blue lines correspond to training signals for ML, and orange variables are outputs of the model. In Figure 1(a) we use the dataset to train a ML forecasting model, the model to predict future exogenous inputs, and use the forecasts *online* for planning optimal action sequences. In Figure 1(b) we design policies which use the dataset to evaluate a policy’s performance, and train π_θ using collected rewards. In Figure 1(c) our approach uses the dataset directly in planning *offline*, and trains a π_θ policy to mimic the actions observed to be optimal on most sample paths.

In this paper, we propose a framework, HINDSIGHT LEARNING, that leverages the above independence structure to reduce the statistical and computational cost of policy learning for MDPs with exogenous inputs (Exo-MDPs). Our framework is based on recent advances in prophet inequalities and hindsight planning [75, 28]. HINDSIGHT LEARNING guides policy search with informative improvement signals computed by *hindsight planning* algorithms developed in the operations research literature [23], which can efficiently solve for the optimal sequence of actions for a given sequence of exogenous inputs. Consequently, our algorithm can quickly learn policies that are “optimal for most exogenous inputs”, which reduces the sample and computational costs of policy search.

Overall, HINDSIGHT LEARNING uses three ingredients, 1) historical data, 2) a hindsight planner, and 3) a high fidelity simulator, to perform policy search, while existing works on Exo-MDPs only uses a subset of these. Figure 1 illustrates the key differences between our approach and prior approaches. For instance, one popular approach (denoted as ML Forecasting) is to predict the exogenous variables using machine learning (ML) and then use the learned model of the exogenous process in policy optimization. Another common approach (denoted as Sim2Real RL) uses the same historical data and the known high-fidelity simulator, like HINDSIGHT LEARNING, but performs policy search by running an off-the-shelf RL algorithm (which acts as a zero-order optimization algorithm). Like Sim2Real RL, HINDSIGHT LEARNING removes the modeling of the exogenous process needed by ML Forecasting, but HINDSIGHT LEARNING does not use RL as the policy optimizer. Instead it leverages the hindsight planner developed by domain experts in operations research and imitation learning to distill the planned results into a single policy, which leads to faster and more reliable convergence as well as more generalizable policies.

Contributions:

1. Through the framework of Exo-MDPs, we bridge the problems studied in operations management and reinforcement learning communities. This connection introduces the possibility of leveraging hindsight planners to help policy optimization.
2. We introduce HINDSIGHT LEARNING for efficient policy optimization in Exo-MDPs. We show that the regret of the hindsight policy (which our approach aims to recover) to the optimal

policy is asymptotically zero or bounded by a novel quantity termed the *hindsight bias*. We show that the hindsight bias, which measures the per-period regret the policy experiences for using the hindsight planner in a non-anticipatory fashion, is a small constant in many problems of practical interest.

3. We develop an imitation learning approach that uses the hindsight optimal actions produced by the hindsight planner on sampled exogenous traces to train a non-anticipatory policy. This approach combines advances in operation management and machine learning. Theoretically, this technique results in better robustness to highly-correlated exogenous distributions, and a better bias-variance trade-off which leads to improved performance in low-data regimes.
4. We also validate our proposed approach numerically in a virtual machine allocation experiment using *real-world* Microsoft Azure traces. The experimental results highlight superior empirical performance of HINDSIGHT LEARNING compared with Sim2Real RL algorithms and domain-specific heuristics. These experiments on real-world clusters also demonstrate the scalability of HINDSIGHT LEARNING.

2 Related Work

There is an extensive literature on reinforcement learning and its connection to tasks in operations management; below, we highlight the work which is closest to ours, but for more extensive references, see [71] for RL, [61] for background on MDPs, and a longer discussion in Appendix B.

Recent research has demonstrated the benefits of incorporating ML advice in designing online algorithms [51, 60, 37]. These techniques have also been explored explicitly in the context of RL. In [56, 39] they use future-conditioned value estimates as control variates in stochastic approximation. This technique was also used by [55] in the resource allocation problems that we study (and is benchmarked in Section 6). Both works build on existing Sim2Real RL algorithms and accelerate their performance by reducing the variance of policy gradient estimates. Our model of Exo-MDPs generalizes several related models in this literature by allowing arbitrary exogenous processes (not just iid) and reward functions (not just additive) [55, 26].

Researchers have investigated new network architectures for use with hindsight planners. [74] consider policies based on Recurrent Neural Networks (RNN) to imitate the hindsight planner. The hope is that the hindsight planner (which uses privileged information) is imitable by using learned recurrent states, and a variational bottleneck can encourage the agent to avoid relying on privileged information. Such RNN policies are used in asymmetric imitation learning [78], hindsight credit assignment [43], and upside-down RL [68, 20], but are often impractical for systems applications.

RL has been applied to variants of resource allocation problems. [53] develop a DeepRM system which can pack tasks with multiple resource demands via a policy gradient method with input driven baselines [55], which we compare against in Section 6. [82] solved a different heterogeneous scheduling problem with deep Q learning. [64] developed a modification of DQN with reward shaping to develop a VM scheduling policy for multi-NUMA machines and motivates the DQN comparisons in our experiments. All of these algorithms modify existing Sim2Real RL algorithms and show empirical gains on variations of the VM scheduling problem. We instead use hindsight planning explicitly during training.

A separate line of work explicitly uses estimates from hindsight planners in algorithm design, however these estimates are overly optimistic. The over-estimation can be rectified by introducing *information penalties* to penalize the planner’s access to future information [75, 15]. This work has

been developed explicitly for some infinite horizon MDPs [15, 30], and constructing these penalties for general problems is an active research area.

3 Preliminaries

3.1 MDPs with Exogenous Inputs (Exo-MDPs)

We consider the finite horizon reinforcement learning setting where an agent is interacting with a Markov decision process (MDP) [61]. The MDP is given by a six-tuple $(\mathcal{S}, \mathcal{A}, T, p, R, s_1)$ where T is the horizon, $(\mathcal{S}, \mathcal{A})$ denotes the set of states and actions, R is the reward distribution, p the distribution governing the transitions of the system, and s_1 is the given starting state. We restrict our attention to non-anticipatory Markov policies $\pi : \mathcal{S} \rightarrow \Delta(\mathcal{A})$ and let Π be the policy class of the learning agent.

We specialize this general model to **MDPs with exogenous inputs** as follows. We assume the decision maker has access to an *endogenous* or *system* state $x \in \mathcal{X}$, where \mathcal{X} is the endogenous state space. Let $\xi = (\xi_1, \dots, \xi_T)$ be a sequence of exogenous inputs with each ξ_t supported on a set Ξ . We assume that ξ is sampled according to an unknown distribution \mathcal{P}_Ξ and that the agent is non-anticipating (i.e. ξ_t is observed only after taking action at time step t). This leads to a state space decomposition $\mathcal{S} := \mathcal{X} \times \Xi^T$ of the MDP, and the system evolves as follows. At time t , the agent selects its action $a_t \in \mathcal{A}$ based solely on the current state $s_t := (x_t, \xi_{<t})$ where $\xi_{<t} = (\xi_1, \dots, \xi_{t-1})$ is the vector of observed exogenous inputs thus far. The endogenous state evolves according to $x_{t+1} = f(s_t, a_t, \xi_t)$, the reward earned is $r(s_t, a_t, \xi_t)$, and ξ_t is observed. We assume the transition dynamics and reward conditioned on the exogenous input $f : \mathcal{S} \times \mathcal{A} \times \Xi \rightarrow \mathcal{X}$ and $r : \mathcal{S} \times \mathcal{A} \times \Xi \rightarrow [0, 1]$ are deterministic.

This model can describe settings where ξ is Markovian, independent across time, or potentially unobserved. See Appendix C for more discussion, a list of examples, and the relationship to prototypical MDP models in RL.

3.2 Value Functions

For a policy $\pi \in \Pi$, the *values* and *action-value* functions are defined according to:

$$V_t^\pi(s) := \mathbb{E}[\sum_{\tau \geq t} r(s_\tau, a_\tau, \xi_\tau) \mid s_t = s] \quad \text{and} \quad Q_t^\pi(s, a) := \mathbb{E}[\sum_{\tau \geq t} r(s_\tau, a_\tau, \xi_\tau) \mid s_t = s, a_t = a]$$

where the expectation is taken over both the randomness in the policy π and the exogenous inputs ξ . We denote π^* as the optimal policy, i.e. the policy that maximizes $V_t^\pi(s)$ in each state s , and denote Q^*, V^* for Q^{π^*}, V^{π^*} respectively. For convenience we assume that $\pi^* \in \Pi$.

Dataset and Regret: We assume the algorithm designer is given access to a dataset $\mathcal{D} = \{\xi^1, \dots, \xi^N\}$ where each trace $\xi^n = \{\xi_1^n, \dots, \xi_T^n\}$ is sampled according to \mathcal{P}_Ξ . The goal is to find a policy $\pi \in \Pi$ that achieves near-optimal expected return $V_1^\pi(s_1)$. Equivalently, we want to output a policy π whose regret $\text{REGRET}(\pi)$ is small, where

$$\text{REGRET}(\pi) := V_1^*(s_1) - V_1^\pi(s_1).$$

3.3 Assumptions

We make the following assumptions which are motivated by our application areas of interest (see Appendix C). We first assume that the only unknown in the MDP is the exogenous process. This assumption is natural for systems applications where the transition model and reward updates the system state according to the exogenous input.

Assumption 1. *The transition model f and reward function r are known to the agent.*

In addition, we assume access to a hindsight planning oracle. In Appendix D we discuss relevant problem domains where such an oracle can be implemented, but note that our training method is *offline* and so the computational burden is not required at run-time (unlike forecasting approaches).

Assumption 2. *Given any trace $\xi_{\geq t} = (\xi_t, \dots, \xi_T)$ and state $s = (x_t, \xi_{<t})$ we can solve:*

$$\begin{aligned} \max_{a_t, \dots, a_T} \quad & \sum_{\tau=t}^T r(s_\tau, a_\tau, \xi_\tau) \\ \text{s.t.} \quad & x_{\tau+1} = f(s_\tau, a_\tau, \xi_\tau), \text{ for } \tau = t, \dots, T \\ & s_\tau = (x_\tau, \xi_{<\tau}), \text{ for } \tau = t, \dots, T. \end{aligned} \tag{1}$$

We denote the optimal objective value to this problem as $\text{HINDSIGHT}(t, \xi_{\geq t}, s)$.

Implementation of the hindsight planner relies on existing techniques from the optimization community. For example, planning problems induced by online knapsack as a function of a deterministic exogenous input sequence can be solved by their induced linear relaxation in pseudo-polynomial time [38]. Other problems, such as inventory control with lead times, have planning problems where a simple greedy control policy is optimal. In general, these problems can be represented as an integer program and use existing heuristics from the optimization literature for efficient solutions [23]. More discussion on this, the use of approximate maximization oracles, and a discussion on our implementation of the hindsight planner for VM allocation is in Appendix D.

3.4 Value Function Decomposition

An important aspect of Exo-MDPs is that value functions can be decomposed into taking expectations over a fixed exogenous trace. Given $\xi = \{\xi_1, \dots, \xi_T\}$ we introduce the value functions for a fixed exogenous sequence ξ and non-anticipatory policy π :

$$Q_t^\pi(s, a, \xi_{\geq t}) := \mathbb{E}\left[\sum_{\tau \geq t} r(s_\tau, a_\tau, \xi_\tau) \mid s_t = s, a_t = a\right] \tag{2}$$

$$V_t^\pi(s, \xi_{\geq t}) := \sum_a \pi(a|s) Q_t^\pi(s, a, \xi_{\geq t}). \tag{3}$$

Note here that the expectation is only taken over the randomness in the policy π , as once ξ is fixed the dynamics and rewards of the system are deterministic.

Lemma 1. *For every $t \in [T]$, $(s, a) \in \mathcal{S} \times \mathcal{A}$, and $\pi \in \Pi$, we have the following:*

$$Q_t^\pi(s, a) = \mathbb{E}_{\xi_{\geq t}}[Q_t^\pi(s, a, \xi_{\geq t})] \tag{4}$$

$$V_t^\pi(s) = \mathbb{E}_{\xi_{\geq t}}[V_t^\pi(s, \xi_{\geq t})]. \tag{5}$$

In particular $V_1^\pi(s_1) = V_1^\pi = \mathbb{E}_\xi[V_1^\pi(s_1, \xi)]$.

The assumptions and the value function decomposition immediately imply the following observations:

No need for Exploration: Given any non-anticipatory deterministic policy π and exogenous trace ξ we can calculate $V_1^\pi(s_1, \xi)$ exactly by evaluating the returns observed when selecting actions according to π with the transition dynamics $x_{t+1} = f(s_t, a_t, \xi_t)$. This means that given a historical dataset, we can have high-fidelity simulation and evaluation of any policy.

Lack of Support Mismatch Issue: A common issue in RL is *support mismatch* where trajectories from the data-collection behavioural policy do not cover the scenarios that the learner policy would visit. However, given even a single trace of ξ sampled according to \mathcal{P}_Ξ , here we have that $V_1^\pi(s_1, \xi)$ is a true unbiased estimate of the value of π .

These two observations suggest that we can train any “online” RL algorithm by simulation that replays “offline” exogenous traces, without worrying about the sim-to-real gap. Furthermore, we can use this property to perform validation on held-out exogenous traces to select hyperparameters without collecting new data, just as in supervised learning.

4 Hindsight Learning in Exo-MDPs

Our HINDSIGHT LEARNING approach (Figure 1(c)) learns a *hindsight planning* surrogate policy, which we denote as π^\dagger :

$$\pi_t^\dagger(s) := \operatorname{argmax}_{a \in \mathcal{A}} Q_t^\dagger(s, a) \quad (6)$$

$$Q_t^\dagger(s, a) := \mathbb{E}_{\xi_{\geq t}} [r(s, a, \xi_t) + \text{HINDSIGHT}(t + 1, \xi_{>t}, f(s, a, \xi_t))] \quad (7)$$

$$V_t^\dagger(s) := \mathbb{E}_{\xi_{\geq t}} [\text{HINDSIGHT}(t, \xi_{\geq t}, s)] \quad (8)$$

Note that π^\dagger is a non-anticipatory, feasible policy, as it only depends on the current state s by taking expectation over future exogenous randomness. We also define $Q_t^\dagger(s, a, \xi_{\geq t})$ and $V_t^\dagger(s, a, \xi_{\geq t})$ as the terms inside of the expectation. This policy is also referred to as the “Bayes Selector” in the literature [75] and has been used on applications from bin packing to refugee resettlement [5, 9]. We can intuitively view π^\dagger as using the value of optimal actions on fixed exogenous traces as scoring signals and selecting actions that are “optimal on most exogenous inputs”.

However, trivially we have that $V_t^\dagger(s) \geq V^*(s)$ and $Q_t^\dagger(s, a) \geq Q^*(s, a)$, and so π^\dagger is necessarily biased for the optimal policy. We derive a regret bound for π^\dagger against π^* by bounding the *hindsight bias*. While suffering the bias term, learning π^\dagger from data is more computationally efficient than learning to approximate π^* when a hindsight planning oracle is available. Because the optimization problem for learning π^\dagger can be reduced to a sequence of regression or classification problems with imitation learning [81], it provides richer signals like gradients than the zero-order information of black-box RL.

We design our algorithm HINDSIGHT LEARNING based on this key observation. At a high level, our HINDSIGHT LEARNING approach seeks to learn π^\dagger using the dataset \mathcal{D} via an imitation learning reduction where the π^\dagger policy is treated as an expert policy. In this way, our algorithm can exploit existing tools for evaluating HINDSIGHT in various domains of interest to speed up the policy search.

We first characterize the regret of π^\dagger and discuss when π^\dagger can have negligible regret, which turns out to include many system applications. Then we give details of our iterative optimization scheme (Algorithm 1) that can efficiently approximate π^\dagger by querying the HINDSIGHT oracle.

4.1 Regret of Hindsight Planning Policy

Before showing the positive results, we first show an example where π^\dagger is arbitrarily bad.

Lemma 2. *There exists a set of Exo-MDPs such that $\text{REGRET}(\pi^\dagger) \geq \Omega(T)$.*

This result highlights that HINDSIGHT LEARNING is not for *every* Exo-MDP. Indeed, to leverage the hindsight planning policy for general Exo-MDPs, the bias needs to be properly controlled, as shown in [16, 30]. These works subtract a baseline $b(s, a, \xi)$ from the rewards when computing the

HINDSIGHT in Equation (6) in order to correct the bias difference between $Q_t^\dagger(s, a)$ and $Q_t^*(s, a)$. However, constructing such baselines in general is difficult.

Nonetheless, a constant regret bound for $\text{REGRET}(\pi^\dagger)$ is actually known for many problems in operations research. Recent work has shown that $\text{REGRET}(\pi^\dagger) = O(1)$ in settings such as online packing, online matching, generalized assignment problems, and secretary problems when mild conditions hold on the tail bounds of the ξ distribution [75, 34, 76]. The performance of the π^\dagger policy has also been studied using prophet inequalities (i.e. regret guarantees against V^\dagger instead of V^*) or competitive ratio [28]. But these results do not characterize the regret of interest here.

Below we derive a new regret bound of π^\dagger in terms of the *hindsight bias*, and show that this gives regret bounds for our surrogate policy π^\dagger scaling as a constant independent of the time horizon. We also outline additional settings where $\pi^\dagger = \pi^*$ or $\text{REGRET}(\pi^\dagger) = O(1)$.

We start by introducing the *hindsight bias* which measures the suboptimality of π^\dagger versus π^* .

Definition 1. *The hindsight bias of π^* versus π^\dagger at time t in state s is defined as*

$$\Delta_t^\dagger(s) := Q_t^\dagger(s, \pi^\dagger(s)) - Q_t^*(s, \pi^\dagger(s)) + Q_t^*(s, \pi^*(s)) - Q_t^\dagger(s, \pi^*(s)). \quad (9)$$

This quantity measures the regret the agent experiences following actions dictated by π^\dagger versus the optimal policy. Below we show that $\Delta_t^\dagger(s)$ provides a natural bound on the regret for the π^\dagger policy.

Lemma 3. $\text{REGRET}(\pi^\dagger) \leq \sum_{t=1}^T \mathbb{E}_{S_t \sim \text{Pr}_t^{\pi^\dagger}} [\Delta_t^\dagger(S_t)]$ where $\text{Pr}_t^{\pi^\dagger}$ denotes the state distribution of π^\dagger at step t induced by the exogenous randomness. In particular, if $\Delta_t^\dagger(s) \leq \Delta$ for some constant Δ then we have:

$$\text{REGRET}(\pi^\dagger) \leq \Delta \sum_{t=1}^T \mathbb{E}_{S_t \sim \text{Pr}_t^{\pi^\dagger}} [\text{Pr}(\pi_t^\dagger(S_t) \neq \pi^*(S_t))].$$

Regret bounds of this form have been shown in the prophet inequality literature [28, 76]. However, typical to this literature is developing guarantees against a stronger benchmark, the hindsight planner, where regret is defined as $\mathbb{E}_\xi [\text{HINDSIGHT}(1, s_1, \xi) - V_1^\pi(s_1, \xi)]$. Our regret decomposition in Lemma 3 is presented similar to compensated coupling arguments but for non-anticipatory policies.

We can use Lemma 3 to show that for several related problems of interest, the regret of π^\dagger is constant independent of the time horizon and scale of the problem. For example, in Lemma 3.1 from [34], the authors show that in stochastic online bin packing with i.i.d. arrivals, $\text{Pr}(\pi_t^\dagger(S_t) \neq \pi_t^*(S_t)) \leq O(\frac{1}{t^2})$. Using a novel absolute bound on Δ we are able to show the following with Lemma 3.

Theorem 4. *In stochastic online bin packing with i.i.d. arrivals we have that $\sup_{t,s} \Delta_t^\dagger(s) \leq O(1)$, independent of the time horizon and any problem primitives. As a result, $\text{REGRET}(\pi^\dagger) \leq O(1)$.*

Developing similar bounds for other systems applications, including inventory control and scheduling problems (such as VM allocation) is an interesting direction for future work.

4.2 Hindsight Learning Algorithms

In the previous section we showed that the hindsight planner policy π^\dagger has $\text{REGRET}(\pi^\dagger) = 0$ or $O(1)$ for many problem domains of interest. However, exactly executing π^\dagger requires frequent calls to the hindsight planning oracle online. This is infeasible for large scale systems applications where the execution of the policy must satisfy latency constraints to ensure quality of service as in VM allocation. In the following we develop our HINDSIGHT LEARNING approach for learning the π^\dagger

Algorithm 1 Hindsight Learning

- 1: **Input:** An empty buffer \mathcal{B} , dynamics models f and r , initial policy π , dataset \mathcal{D} .
 - 2: **for** $k = 1, 2, \dots, K$ **do**
 - 3: Sample a trace ξ from \mathcal{D}
 - 4: Sample trajectories using the current policy π using the known dynamics f and reward function r over the exogenous trace ξ
 - 5: Query hindsight planning oracle to label the sampled trajectories with $\{Q_t^\dagger(s_t, a, \xi_{\geq t}) : a \in \mathcal{A}, t \in [T]\}$
 - 6: Aggregate the labeled data into a buffer \mathcal{B}
 - 7: Optimize the policy by either HINDSIGHT MAC objective in (10) or HINDSIGHT Q-DISTILLATION objective in (11) on \mathcal{B}
 - 8: **end for**
-

policy using deep learning. It performs all computation and hindsight planning oracle calls offline to allow the learned policy to have low latency, and appeals to generalization to allow the learned policies to extrapolate to unseen parts of the state space.

To this end, we leverage the framework of online imitation learning (IL) [62], which is a powerful technique for learning to search. Specifically, we can treat π^\dagger as an expert policy in IL for which we can query for value functions $Q^\dagger(s, a)$ through the hindsight planning oracles. This is summarized in Algorithm 1, where we interleave the policy trajectory sampling and updates to avoid the need of querying $Q^\dagger(s, a)$ for all states and actions.

Under standard no-regret optimization and policy realizabilty assumptions of online IL, the performance of the best policy produced by Algorithm 1 would converge to that of π^\dagger . [70, 62, 81]. Here we present results using the overline notation to correspond to quantities with respect to the empirical MDP whose exogenous distribution \mathcal{P}_Ξ is replaced with the empirical one $\overline{\mathcal{P}}_\Xi$ from \mathcal{D} .

Theorem 5. *Let $\overline{\pi}^\dagger$ denote the hindsight planning surrogate policy for the empirical MDP w.r.t. \mathcal{D} . Assume $\overline{\pi}^\dagger \in \Pi$ and Algorithm 1 achieves no-regret in the optimization problem. Let π be the best policy generated by Algorithm 1. Then, for any $\delta \in (0, 1)$, with probability $1 - \delta$, it holds*

$$\text{REGRET}(\pi) \leq 2T \sqrt{\frac{2 \log(2|\Pi|/\delta)}{N}} + \sum_{t=1}^T \mathbb{E}_{S_t \sim \overline{P}_{r_t}^{\overline{\pi}^\dagger}} [\overline{\Delta}_t^\dagger(S_t)] + o(1)$$

for $\overline{\Delta}_t^\dagger$ the SAA approximation of (9), and $\overline{P}_{r_t}^{\overline{\pi}^\dagger}$ is the state probability in the empirical MDP.

Theorem 5 shows that Algorithm 1 functions as an iterative optimization procedure to maximize the return in the empirical MDP. Algorithm 1 performs IL in this empirical MDP to achieve faster optimization [81] than Sim2Real RL. However, it pays for the empirical hindsight bias $\overline{\pi}^\dagger$ for this faster optimization. We see that $\mathbb{E}_{\overline{P}_{r_t}^{\overline{\pi}^\dagger}} [\overline{\Delta}_t^\dagger(S_t)] \leq 0$ when $|\mathcal{D}| = 1$ and $\sum_{t=1}^T \mathbb{E}_{\overline{P}_{r_t}^{\overline{\pi}^\dagger}} [\overline{\Delta}_t^\dagger(S_t)] \rightarrow \sum_{t=1}^T \mathbb{E}_{P_{r_t}^{\pi^\dagger}} [\Delta_t^\dagger(S_t)] = O(1)$ as we collect more exogenous traces. Therefore, although we do not have a statistical rate on empirical hindsight bias, we conjecture that it is likely to be no larger than the population counterpart, which is constant for practical problems.

To conclude this section, we give two examples of Algorithm 1 below: one using policy network design and the other with a critic network. In general, our approach suggests replacing Monte Carlo estimates of the current $Q^\pi(s, a)$ value in any RL algorithm with the hindsight estimate $Q^\dagger(s, a)$.

4.2.1 Hindsight MAC

The first algorithm we present is a variant of the Mean Actor Critic algorithm [6] and inspired by differentiable imitation learning techniques with policy networks [70]. We use a neural network representation for the policy class via $\Pi = \Pi_\Theta$. Consider the loss function for the currently chosen policy π :

$$\ell(\pi_\theta) = \mathbb{E}_\xi \left[\sum_{t=1}^T \mathbb{E}_{S_t \sim \text{Pr}_t^\pi} \sum_{a \in \mathcal{A}} \pi_\theta(a | S_t) Q_t^\dagger(S_t, a, \xi_{\geq t}) \right]. \quad (10)$$

This loss function encourages the policy that maximizes the planning policies reward-to-go under the state distribution from the current learned policy π , and exploits the ability to simulate and obtain $Q_t^\dagger(s, a, \xi_{\geq t})$ values for any action $a \in \mathcal{A}$.

4.2.2 Hindsight Q-Distillation

The second algorithm uses a neural network representation for the critic class and derives an approximate π^\dagger indirectly. Set Q^Θ to be the set of potential Q functions parameterized by the parameter set Θ . The policy employed is then $\pi_\theta = \text{argmax}_{a \in \mathcal{A}} Q_t^\theta(s, a)$.

We calculate the loss function $\ell(\pi_\theta)$ to ensure that $Q_t^\theta(s, a)$ is fit to $Q_t^\dagger(s, a)$ as follows:

$$\mathbb{E}_\xi \left[\sum_{t=1}^T \mathbb{E}_{S_t \sim \text{Pr}_t^\pi} \left[\sum_{a \in \mathcal{A}} (Q_t^\theta(S_t, a) - Q_t^\dagger(S_t, a, \xi_{\geq t}))^2 \right] \right]. \quad (11)$$

5 Existing Approaches to MDPs in Exo-MDPs

Here we briefly discuss existing approaches to MDPs applied in the context of Exo-MDPs to highlight the advantages and disadvantages of the HINDSIGHT LEARNING approach.

5.1 Decision-Making using ML Forecasts

Given the historical trace dataset $\mathcal{D} = \{\xi^1, \dots, \xi^N\}$, a popular plug-in approach learns a generative model $\overline{\mathcal{P}}_\Xi(\xi_t | \xi_{<t})$ to approximate the true distribution $\mathcal{P}_\Xi(\xi_t | \xi_{<t})$, since the exogenous process is the only unknown. Given this model $\overline{\mathcal{P}}_\Xi$, estimates for the Q_t^* value for the optimal policy can be obtained by solving the Bellman equation with the learned predictor $\overline{\mathcal{P}}_\Xi$ in place of the true distribution \mathcal{P}_Ξ . More concretely, we denote \overline{Q}_t as the model-based estimate of Q_t^* , which follows

$$\begin{aligned} \overline{Q}_t(s, a) &:= \mathbb{E}_{\xi | \xi_{<t}} [r(x, a, \xi) + \overline{V}_{t+1}(f(x, a, \xi) | \overline{\mathcal{P}}_\Xi)] \\ \overline{V}_t(s) &:= \max_{a \in \mathcal{A}} \overline{Q}_t(s, a) \\ \overline{\pi}_t(s) &:= \text{argmax}_{a \in \mathcal{A}} \overline{Q}_t(s, a). \end{aligned}$$

While intuitive, this ML forecast approach requires high-fidelity modeling of the exogenous process to guarantee good downstream decision-making, due to the quadratic horizon multiplicative factor in regret we show below. This quadratic factor in the horizon is due to the compounding errors of distribution shift, similar to those shown in the imitation learning literature [62].

Theorem 6. *Suppose that $\sup_{t \in [T], \xi_{<t} \in \Xi^{[t-1]}} \|\overline{\mathcal{P}}_\Xi(\cdot | \xi_{<t}) - \mathcal{P}_\Xi(\cdot | \xi_{<t})\|_{TV} \leq \epsilon$ where $\|\cdot\|_{TV}$ is the total variation distance. Then we have that $\text{REGRET}(\overline{\pi}) \leq 2T^2\epsilon$. In addition, if $\xi \sim \mathcal{P}_\Xi$ has each ξ_t*

independent from $\xi_{<t}$, $\overline{\mathcal{P}}_{\Xi}$ is the empirical distribution, then $\forall \delta \in (0, 1)$, with probability at least $1 - \delta$,

$$\text{REGRET}(\overline{\pi}) \leq 2T^2 \sqrt{\frac{\log(2|\Xi|/\delta)}{N}}.$$

The T^2 dependence here is tight (see [27]), in contrast to the $O(T)$ dependence in Theorem 5. Moreover, the ML forecast approach can be impractical when the exogenous process is complex, such as VM allocation where researchers observed that the VM lifetime varies substantially across time, the demand has spikes and a diurnal pattern, and that subsequent requests are highly correlated [41].

This discrepancy highlights an advantage of our HINDSIGHT LEARNING approach. Consider a VM allocation example with two physical machines each large enough to satisfy the entire demand. Under chaotic and unpredictable arrivals, a planner using erroneous forecasts might spread the requests over the two machines. In contrast, the hindsight learning policy will correctly learn that one machine is sufficient and achieve low regret, even if the total variation distance on the underlying distribution over exogenous inputs is large.

5.2 Stochastic Approximation using Sim2Real RL

Recall that our objective is to solve $\text{argmax}_{\pi \in \Pi} V_1^\pi(s_0)$. This can be written as $\text{argmax}_{\pi \in \Pi} \mathbb{E}_{\xi} [V_1^\pi(s_0, \xi)]$ by Lemma 1. Therefore, an alternative way to find approximately optimal policies for an Exo-MDP is to maximize the empirical return directly, similar to the empirical risk minimization strategy of supervised learning: $\overline{\pi}^* = \text{argmax}_{\pi \in \Pi} \overline{\mathbb{E}}[V_1^\pi(s_0, \xi)]$ where $\overline{\mathbb{E}}[V_1^\pi(s_0, \xi)] = \frac{1}{N} \sum_n V_1^\pi(s_0, \xi^n)$. First observe that the number of samples required to learn a near optimal policy scales linearly with T in this approach. If an additive control variate $\phi(\xi)$ (as in [55]) is used, the T term is replaced with $T - \mathbb{E}_{\xi}[\phi(\xi)]$.

Theorem 7. *For any $\delta \in (0, 1)$, with probability at least $1 - \delta$ we have that*

$$\text{REGRET}(\overline{\pi}^*) \leq T \sqrt{\frac{2 \log(2|\Pi|/\delta)}{N}}.$$

At first glance, Theorem 7 is better than Theorem 5 since it is asymptotically efficient in the large data regime. However, typical Exo-MDP applications are not in the large N regime, so a proper bias-variance trade-off is important (which is difficult to quantify theoretically). For the VM allocation example considered in Section 6, we have minimal data in the trace training set. Sim2Real RL must successfully generalize these few N traces to the true exogenous distribution.

6 Numerical Results

We evaluate our HINDSIGHT LEARNING framework using real-world data for Virtual Machine (VM) allocation. We compare our algorithm’s performance against several baselines, including Sim2Real RL with and without exogenous-dependent control variates [55], and domain-specific heuristics. See Appendix E for details on hyperparameter tuning, network design, and the training procedure.

Note that the ML forecasting approach of predicting the exogenous distribution for downstream optimization is intractable for this scenario. The VM request distribution is irregularly correlated [41], so it is near-impossible to learn an accurate enough predictor of the exogenous trace. However, Sim2Real RL with infinite compute is essentially planning in the empirical MDP to either global or local optimality, so the RL results can be interpreted as a proxy for this algorithm. We recognize that other problem domains admit forecasting baselines, and discuss this more in Appendix E.

Table 1: Performance of heuristics, Sim2Real RL, and HINDSIGHT LEARNING algorithms on VM allocation against the Best Fit baseline. Asterisks indicate significance by Welch’s t -test.

Algorithm	PMs Saved
Performance Upper Bound	4.96*
Best Fit	0.0
Bin Packing	-1.05*
Round Robin	-1.24*
Random	-1.87*
DQN	-0.64
MAC	-0.51*
AC	-0.50
PG with Hindsight Baseline [55]	-0.057
Hindsight MAC	4.33*
HINDSIGHT Q-DISTILLATION	3.71*

6.1 Virtual Machine Allocation for Microsoft Azure

Cloud service providers, such as Microsoft Azure, allows users easy access to computing resources. The most critical component, the *cluster allocator*, assigns a given Virtual Machine (VM) request to the physical hardware, henceforth referred to as a Physical Machine (PM). Each VM request has an associated lifetime, CPU requirement, and memory requirement. The allocator must assign physical resources to arriving VM requests efficiently by eliminating fragmentation, performance impacts, and allocation failures.

These VM allocation problems are a multi-dimensional variant of online bin-packing with stochastic arrivals and departures. While there are no known bounds on the hindsight bias, we note that the empirical evidence of hindsight learning inspires future work in OR and RL to derive hindsight bias bounds for other problems. Moreover, the simplified problem with known lifetimes lasting until the entire time horizon and only one dimension reduces to the online bin-packing problem in Theorem 4 where we derive a constant hindsight bias regret bound.

We conduct our experiments using the open-source simulator MARO [46]. The public dataset contains VM requests uniformly sampled from 2019 historical Microsoft Azure workloads, and measures the performance for the allocator decisions on the *JP1* cluster containing 80 PMs in the *Asia Northeast* availability zone.

By default, MARO provides reward metrics that can be used when assessing an algorithm such as income, energy consumption, and failed allocations. However, the default approach for building resilient infrastructure is over-provisioning, so any reasonable allocation policy is able to allocate every VM to a PM (see Figure 3(a) for a trace of historical demand). We instead use:

$$r(s, a, \xi) = -1/\text{Packing-Density}(s). \tag{12}$$

The packing density is computed as the ratio of used cores over the core capacity for all physical machines that are utilized. A measure of one corresponds to the current running VMs using exactly the total capacity of all used physical machines. This serves to differentiate algorithms by measuring their ability to pack the VMs in a minimal number of PMs as possible. It is also cited as a key efficiency metric as CPU cores are typically the bottleneck resource [41]. See Figure 4 for an illustration. However, for interpretability of the experimental results in Table 1 we include the

average difference in PMs required to service the load. See Table 4 for results on the true $r(s, a, \xi)$ values and the packing density.

Training Procedure: To evaluate the trained policies we subdivided a one-month trace from the 2019 historical Microsoft Azure dataset into a training and test portion. For evaluation we sampled 50 different one-day traces of VM requests from the held-out portion. See Appendix E for more details.

6.2 Main Results

In Table 1 we show a comparison of the performance for the various algorithms on the average number of PMs required to service the load. The first row corresponds to the optimal hindsight planning values on the heldout exogenous traces, and serves as an upper bound on the performance of *any* algorithm. The performance for **Best Fit** is zero as the values presented are the difference against this policy. Mean Actor-Critic (MAC) [6] is a variant of Actor-Critic that uses Q^π for all actions during policy improvement, while Policy Gradient uses a future-conditioned baseline [55]. For a full description of the Sim2Real RL algorithms and heuristics see Appendix E.

We see that the HINDSIGHT LEARNING algorithms are able to outperform all of the heuristics and Sim2Real RL algorithms. We also note that the improvement of 4.33 fewer PMs required to service the load implies that HINDSIGHT MAC requires 5% fewer PMs on average. As each algorithm had access to the same amount of training data, this shows that the HINDSIGHT LEARNING algorithms witness a statistical benefit versus blackbox algorithms in this low data regime. Moreover, the computational footprint for training across the different algorithms are comparable. The learning curves presented in Figure 5 show that the training losses converged for each algorithm. This highlights that all of the RL algorithms converged within the same computational budget, and that the HINDSIGHT LEARNING algorithms show empirical statistical benefits.

Acknowledgements

Part of this work was done while Sean Sinclair was a research intern at Microsoft Research, and a visitor at Simons Institute for the semester on the Theory of Reinforcement Learning. We also gratefully acknowledge funding from the NSF under grants ECCS-1847393, DMS-1839346, CCF-1948256, and CNS-1955997, and the ARL under grant W911NF-17-1-0094.

References

- [1] Pieter Abbeel and Andrew Y Ng. Exploration and apprenticeship learning in reinforcement learning. In *ICML*, pages 1–8, 2005.
- [2] Jacob Abernethy, Peter L Bartlett, Niv Buchbinder, and Isabelle Stanton. A regularization approach to metrical task systems. In *ALT*, pages 270–284, 2010.
- [3] Alekh Agarwal, Nan Jiang, Sham M Kakade, and Wen Sun. Reinforcement Learning: Theory and Algorithms. *UW Seattle Tech. Rep.*, page 172, 2019.
- [4] Shipra Agrawal and Randy Jia. Learning in structured mdps with convex cost functions: Improved regret bounds for inventory management. In *EC*, pages 743–744, 2019.
- [5] Narges Ahani, Paul Gözl, Ariel D Procaccia, Alexander Teytelboym, and Andrew C Trapp. Dynamic placement in refugee resettlement. *arXiv preprint arXiv:2105.14388*, 2021.

- [6] Cameron Allen, Kavosh Asadi, Melrose Roderick, Abdel-rahman Mohamed, George Konidaris, and Michael Littman. Mean actor critic. *arXiv preprint arXiv:1709.00503*, 2017.
- [7] Thomas Anthony, Zheng Tian, and David Barber. Thinking fast and slow with deep learning and tree search. In *NeurIPS*, pages 5366–5376, 2017.
- [8] Santiago R Balseiro and David B Brown. Approximations to stochastic dynamic programs via information relaxation duality. *Operations Research*, 67(2):577–597, 2019.
- [9] Siddhartha Banerjee and Daniel Freund. Uniform loss algorithms for online stochastic decision-making with applications to bin packing. In *Abstracts of the 2020 SIGMETRICS/Performance Joint International Conference on Measurement and Modeling of Computer Systems*, pages 1–2, 2020.
- [10] Irwan Bello, Hieu Pham, Quoc V Le, Mohammad Norouzi, and Samy Bengio. Neural combinatorial optimization with reinforcement learning. In *ICLR*, 2017.
- [11] Dimitris Bertsimas and John N Tsitsiklis. *Introduction to linear optimization*, volume 6. Athena Scientific Belmont, MA, 1997.
- [12] Christian Borgs, Jennifer T Chayes, László Lovász, Vera T Sós, and Katalin Vesztegombi. Convergent sequences of dense graphs i: Subgraph frequencies, metric properties and testing. *Advances in Mathematics*, 219(6):1801–1851, 2008.
- [13] Allan Borodin, Nathan Linial, and Michael E Saks. An optimal on-line algorithm for metrical task system. *Journal of the ACM (JACM)*, 39(4):745–763, 1992.
- [14] Luce Brotcorne, Gilbert Laporte, and Frédéric Semet. Ambulance location and relocation models. *European Journal of Operational Research*, 147(3):451–463, June 2003.
- [15] David B Brown and Martin B Haugh. Information relaxation bounds for infinite horizon markov decision processes. *Operations Research*, 65(5):1355–1379, 2017.
- [16] David B Brown and James E Smith. Information relaxations, duality, and convex stochastic dynamic programs. *Operations Research*, 62(6):1394–1415, 2014.
- [17] David B Brown and James E Smith. Information relaxations and duality in stochastic dynamic programs: A review and tutorial. 2021.
- [18] Sébastien Bubeck, Nicolo Cesa-Bianchi, and others. Regret analysis of stochastic and non-stochastic multi-armed bandit problems. *Foundations and Trends in Machine Learning*, 5(1):1–122, 2012. Publisher: Now Publishers, Inc.
- [19] Dong Chen, Zhaojian Li, Tianshu Chu, Rui Yao, Feng Qiu, and Kaixiang Lin. Power-net: Multi-agent deep reinforcement learning for scalable powergrid control. *arXiv preprint arXiv:2011.12354*, 2020.
- [20] Lili Chen, Kevin Lu, Aravind Rajeswaran, Kimin Lee, Aditya Grover, Michael Laskin, Pieter Abbeel, Aravind Srinivas, and Igor Mordatch. Decision transformer: Reinforcement learning via sequence modeling. *arXiv preprint arXiv:2106.01345*, 2021.
- [21] Rohan Chitnis and Tomás Lozano-Pérez. Learning compact models for planning with exogenous processes. In *Conference on Robot Learning*, pages 813–822. PMLR, 2020.

- [22] Christian Coester and Elias Koutsoupias. Towards the k-server conjecture: A unifying potential, pushing the frontier to the circle. *arXiv preprint arXiv:2102.10474*, 2021.
- [23] Michele Conforti, Gérard Cornuéjols, Giacomo Zambelli, et al. *Integer programming*, volume 271. Springer, 2014.
- [24] Eli Cortez, Anand Bonde, Alexandre Muzio, Mark Russinovich, Marcus Fontoura, and Ricardo Bianchini. Resource central: Understanding and predicting workloads for improved resource management in large cloud platforms. In *Proceedings of the 26th Symposium on Operating Systems Principles*, pages 153–167, 2017.
- [25] Jim G Dai and Mark Gluzman. Queueing network controls via deep reinforcement learning. *Stochastic Systems*, 2021.
- [26] Thomas Dietterich, George Trimonias, and Zhitang Chen. Discovering and Removing Exogenous State Variables and Rewards for Reinforcement Learning. In *International Conference on Machine Learning*, pages 1262–1270. PMLR, July 2018. ISSN: 2640-3498.
- [27] Omar Darwiche Domingues, Pierre Ménard, Emilie Kaufmann, and Michal Valko. Episodic reinforcement learning in finite mdps: Minimax lower bounds revisited. In *Algorithmic Learning Theory*, pages 578–598. PMLR, 2021.
- [28] Paul Dutting, Michal Feldman, Thomas Kesselheim, and Brendan Lucier. Prophet inequalities made easy: Stochastic optimization by pricing nonstochastic inputs. *SIAM Journal on Computing*, 49(3):540–582, 2020.
- [29] Yonathan Efroni, Dylan J Foster, Dipendra Misra, Akshay Krishnamurthy, and John Langford. Sample-efficient reinforcement learning in the presence of exogenous information. *arXiv preprint arXiv:2206.04282*, 2022.
- [30] Ibrahim El Shar and Daniel Jiang. Lookahead-bounded q-learning. In *International Conference on Machine Learning*, pages 8665–8675. PMLR, 2020.
- [31] Joyce Fang, Martin Ellis, Bin Li, Siyao Liu, Yasaman Hosseinkashi, Michael Revow, Albert Sadvnikov, Ziyuan Liu, Peng Cheng, Sachin Ashok, et al. Reinforcement learning for bandwidth estimation and congestion control in real-time communications. *arXiv preprint arXiv:1912.02222*, 2019.
- [32] Eugene A Feinberg. Optimality conditions for inventory control. In *Optimization Challenges in Complex, Networked and Risky Systems*, pages 14–45. INFORMS, 2016.
- [33] Jiekun Feng, Mark Gluzman, and Jim G Dai. Scalable deep reinforcement learning for ride-hailing. In *2021 American Control Conference (ACC)*, pages 3743–3748. IEEE, 2021.
- [34] Daniel Freund and Siddhartha Banerjee. Good prophets know when the end is near. SSRN Scholarly Paper ID 3479189, Social Science Research Network, Rochester, NY, November 2019.
- [35] Javad Ghaderi, Yuan Zhong, and Rayadurgam Srikant. Asymptotic optimality of bestfit for stochastic bin packing. *ACM SIGMETRICS Performance Evaluation Review*, 42(2):64–66, 2014.
- [36] David A. Goldberg, Martin I. Reiman, and Qiong Wang. A Survey of Recent Progress in the Asymptotic Analysis of Inventory Systems. *Production and Operations Management*, 30(6):1718–1750, 2021.

- [37] Sreenivas Gollapudi and Debmalya Panigrahi. Online algorithms for rent-or-buy with expert advice. In *International Conference on Machine Learning*, pages 2319–2327, 2019.
- [38] Parikshit Gopalan, Adam Klivans, and Raghu Meka. Polynomial-time approximation schemes for knapsack and related counting problems using branching programs. *arXiv preprint arXiv:1008.3187*, 2010.
- [39] Jiaming Guo, Rui Zhang, Xishan Zhang, Shaohui Peng, Qi Yi, Zidong Du, Xing Hu, Qi Guo, and Yunji Chen. Hindsight value function for variance reduction in stochastic dynamic environment. *arXiv preprint arXiv:2107.12216*, 2021.
- [40] Varun Gupta and Ana Radovanovic. Online stochastic bin packing. *arXiv preprint arXiv:1211.2687*, 2012.
- [41] Ori Hadary, Luke Marshall, Ishai Menache, Abhisek Pan, Esaias E Greeff, David Dion, Star Dorminey, Shailesh Joshi, Yang Chen, Mark Russinovich, et al. Protean: {VM} allocation service at scale. In *14th {USENIX} Symposium on Operating Systems Design and Implementation ({OSDI} 20)*, pages 845–861, 2020.
- [42] Pavithra Harsha, Ashish Jagmohan, Jayant Kalagnanam, Brian Quanz, and Divya Singhvi. Math programming based reinforcement learning for multi-echelon inventory management. In *Deep RL Workshop NeurIPS 2021*, 2021.
- [43] Anna Harutyunyan, Will Dabney, Thomas Mesnard, Mohammad Gheshlaghi Azar, Bilal Piot, Nicolas Heess, Hado P van Hasselt, Gregory Wayne, Satinder Singh, Doina Precup, et al. Hindsight credit assignment. *Advances in neural information processing systems*, 32:12488–12497, 2019.
- [44] Haoyuan Hu, Xiaodong Zhang, Xiaowei Yan, Longfei Wang, and Yinghui Xu. Solving a new 3d bin packing problem with deep reinforcement learning method. *arXiv preprint arXiv:1708.05930*, 2017.
- [45] Christian D Hubbs, Hector D Perez, Owais Sarwar, Nikolaos V Sahinidis, Ignacio E Grossmann, and John M Wassick. Or-gym: A reinforcement learning library for operations research problems. *arXiv preprint arXiv:2008.06319*, 2020.
- [46] Arthur Jiang, Jia Zhang, Pingchao Yu, Lyuchun Huang, Yang Qiu, Jinyu Wang, Wenlei Shi, Kaiqi Li, Zhanyu Wang, Chengruidong Zhang, Tianyi Sun, Miaoran Chen, Kuanwei Yu, Xinran Wei, Michael Li, Ning Shang, Qiwei Meng, Shan Li, Jiang Bian, Biao Cheng, and Tie-Yan Liu. Maro: A multi-agent resource optimization platform, 2020.
- [47] Nathan Kallus and Angela Zhou. Stateful offline contextual policy evaluation and learning. *arXiv preprint arXiv:2110.10081*, 2021.
- [48] Vijay R Konda and John N Tsitsiklis. Actor-critic algorithms. In *Advances in neural information processing systems*, pages 1008–1014, 2000.
- [49] Yusen Li, Xueyan Tang, and Wentong Cai. Dynamic bin packing for on-demand cloud resource allocation. *IEEE Transactions on Parallel and Distributed Systems*, 27(1):157–170, 2015.
- [50] László Lovász and Balázs Szegedy. Limits of dense graph sequences. *Journal of Combinatorial Theory, Series B*, 96(6):933–957, 2006.

- [51] Thodoris Lykouris and Sergei Vassilvtiskii. Competitive caching with machine learned advice. In *International Conference on Machine Learning*, pages 3296–3305, 2018.
- [52] Mark S Manasse, Lyle A McGeoch, and Daniel D Sleator. Competitive algorithms for server problems. *Journal of Algorithms*, 11(2):208–230, 1990.
- [53] Hongzi Mao, Mohammad Alizadeh, Ishai Menache, and Srikanth Kandula. Resource management with deep reinforcement learning. In *Proceedings of the 15th ACM workshop on hot topics in networks*, pages 50–56, 2016.
- [54] Hongzi Mao, Malte Schwarzkopf, Shaileshh Bojja Venkatakrisnan, Zili Meng, and Mohammad Alizadeh. Learning scheduling algorithms for data processing clusters. In *Proceedings of the ACM Special Interest Group on Data Communication*, pages 270–288, 2019.
- [55] Hongzi Mao, Shaileshh Bojja Venkatakrisnan, Malte Schwarzkopf, and Mohammad Alizadeh. Variance Reduction for Reinforcement Learning in Input-Driven Environments. *arXiv:1807.02264 [cs, stat]*, February 2019. arXiv: 1807.02264.
- [56] Thomas Mesnard, Theophane Weber, Fabio Viola, Shantanu Thakoor, Alaa Saade, Anna Harutyunyan, Will Dabney, Thomas S. Stepleton, Nicolas Heess, Arthur Guez, Eric Moulines, Marcus Hutter, Lars Buesing, and Remi Munos. Counterfactual Credit Assignment in Model-Free Reinforcement Learning. In *International Conference on Machine Learning*, pages 7654–7664. PMLR, July 2021. ISSN: 2640-3498.
- [57] Adam Paszke, Sam Gross, Francisco Massa, Adam Lerer, James Bradbury, Gregory Chanan, Trevor Killeen, Zeming Lin, Natalia Gimelshein, Luca Antiga, Alban Desmaison, Andreas Köpf, Edward Yang, Zach DeVito, Martin Raison, Alykhan Tejani, Sasank Chilamkurthy, Benoit Steiner, Lu Fang, Junjie Bai, and Soumith Chintala. Pytorch: An imperative style, high-performance deep learning library, 2019. cite arxiv:1912.01703.
- [58] Guido Perboli, Roberto Tadei, and Mauro M Baldi. The stochastic generalized bin packing problem. *Discrete Applied Mathematics*, 160(7-8):1291–1297, 2012.
- [59] Warren Powell. *Reinforcement Learning and Stochastic Optimization: A unified framework for sequential decisions*. Wiley-Interscience, 2020.
- [60] Manish Purohit, Zoya Svitkina, and Ravi Kumar. Improving online algorithms via ml predictions. *Advances in Neural Information Processing Systems*, 31:9661–9670, 2018.
- [61] Martin L. Puterman. *Markov Decision Processes: Discrete Stochastic Dynamic Programming*. John Wiley & Sons, Inc., New York, NY, USA, 1st edition, 1994.
- [62] Stéphane Ross, Geoffrey Gordon, and Drew Bagnell. A reduction of imitation learning and structured prediction to no-regret online learning. In *Proceedings of the fourteenth international conference on artificial intelligence and statistics*, pages 627–635. JMLR Workshop and Conference Proceedings, 2011.
- [63] Junjie Sheng, Shengliang Cai, Haochuan Cui, Wenhao Li, Yun Hua, Bo Jin, Wenli Zhou, Yiqiu Hu, Lei Zhu, Qian Peng, et al. Vmagent: Scheduling simulator for reinforcement learning. *arXiv preprint arXiv:2112.04785*, 2021.

- [64] Junjie Sheng, Yiqiu Hu, Wenli Zhou, Lei Zhu, Bo Jin, Jun Wang, and Xiangfeng Wang. Learning to schedule multi- numa virtual machines via reinforcement learning. *Pattern Recognition*, 121:108254, 2022.
- [65] Sean R. Sinclair, Siddhartha Banerjee, and Christina Lee Yu. Adaptive Discretization for Episodic Reinforcement Learning in Metric Spaces. *Proceedings of the ACM on Measurement and Analysis of Computing Systems*, 3(3):1–44, December 2019. arXiv: 1910.08151.
- [66] Aleksandrs Slivkins. Introduction to Multi-Armed Bandits. *arXiv:1904.07272 [cs, stat]*, September 2019. arXiv: 1904.07272.
- [67] Jialin Song, Ravi Lanka, Albert Zhao, Aadyot Bhatnagar, Yisong Yue, and Masahiro Ono. Learning to search via retrospective imitation. *arXiv preprint arXiv:1804.00846*, 2018.
- [68] Rupesh Kumar Srivastava, Pranav Shyam, Filipe Mutz, Wojciech Jaśkowski, and Jürgen Schmidhuber. Training agents using upside-down reinforcement learning. *arXiv preprint arXiv:1912.02877*, 2019.
- [69] Alexander L Stolyar. An infinite server system with general packing constraints. *Operations Research*, 61(5):1200–1217, 2013.
- [70] Wen Sun, Arun Venkatraman, Geoffrey J Gordon, Byron Boots, and J Andrew Bagnell. Deeply aggregated: Differentiable imitation learning for sequential prediction. In *International Conference on Machine Learning*, pages 3309–3318. PMLR, 2017.
- [71] Richard S. Sutton and Andrew G. Barto. *Reinforcement learning: an introduction*. Adaptive computation and machine learning series. The MIT Press, Cambridge, Massachusetts, second edition edition, 2018.
- [72] Yunhao Tang, Shipra Agrawal, and Yuri Faenza. Reinforcement learning for integer programming: Learning to cut. In *International Conference on Machine Learning*, pages 9367–9376. PMLR, 2020.
- [73] Hado Van Hasselt, Arthur Guez, and David Silver. Deep reinforcement learning with double q-learning. In *Proceedings of the AAAI conference on artificial intelligence*, 2016.
- [74] David Venuto, Elaine Lau, Doina Precup, and Ofir Nachum. Policy Gradients Incorporating the Future. *arXiv:2108.02096 [cs]*, August 2021. arXiv: 2108.02096.
- [75] Alberto Vera and Siddhartha Banerjee. The bayesian prophet: A low-regret framework for online decision making. *Management Science*, 67(3):1368–1391, 2021.
- [76] Alberto Vera, Siddhartha Banerjee, and Itai Gurvich. Online allocation and pricing: Constant regret via bellman inequalities. *Operations Research*, 2021.
- [77] Oriol Vinyals, Meire Fortunato, and Navdeep Jaitly. Pointer networks. *arXiv preprint arXiv:1506.03134*, 2015.
- [78] Andrew Warrington, Jonathan W Lavington, Adam Scibior, Mark Schmidt, and Frank Wood. Robust asymmetric learning in pomdps. In *International Conference on Machine Learning*, pages 11013–11023. PMLR, 2021.
- [79] Martin L Weitzman. Optimal search for the best alternative. *Econometrica: Journal of the Econometric Society*, pages 641–654, 1979.

- [80] Linwei Xin and David A Goldberg. Distributionally robust inventory control when demand is a martingale. *arXiv preprint arXiv:1511.09437*, 2015.
- [81] Xinyan Yan, Byron Boots, and Ching-An Cheng. Explaining fast improvement in online imitation learning. In *Uncertainty in Artificial Intelligence*, pages 1874–1884. PMLR, 2021.
- [82] Haitao Zhang, Xin Geng, and Huadong Ma. Learning-driven interference-aware workload parallelization for streaming applications in heterogeneous cluster. *IEEE Transactions on Parallel and Distributed Systems*, 32(1):1–15, 2020.

A Table of Notation

Symbol	Definition
Problem Setting Specification	
$\mathcal{S}, \mathcal{A}, T, s_1, R, p$	MDP primitives: state and action space, time horizon, starting state
\mathcal{X}	Endogenous space for the system
Ξ	Exogenous input space
\mathcal{P}_Ξ	Distribution over exogenous inputs
$f(s, a, \xi), r(s, a, \xi)$	Underlying deterministic transition and reward as function of exogenous input
s_t	MDP state space primitive $(x_t, \xi_{<t})$ for shorthand
s_t, a_t, ξ_t	State, action, and exogenous input for time step t
ξ	An exogenous input trace (ξ_1, \dots, ξ_T)
$\xi_{\geq t}$	Component of an exogenous input trace (ξ_t, \dots, ξ_T)
Π	Set of all admissible policies
$Q_t^\pi(s, a), V_t^\pi(s)$	Q -Function and value function for policy π at time step t
$\pi^*, Q_t^*(s, a), V_t^*(s)$	Optimal policy and the Q and value function for the optimal policy
Pr_t^π	State-visitation distribution for policy π at time step t
\mathcal{D}	Dataset containing N traces of exogenous inputs $\{\xi^1, \dots, \xi^N\}$
$\text{HINDSIGHT}(t, s, \xi_{\geq t}, f, r)$	Hindsight optimal cumulative reward r starting in state s at time t with exogenous inputs dictated by $\xi_{\geq t}$ and dynamics f (see Equation (1))
$Q_t^\pi(s, a, \xi_{\geq t}), V_t^\pi(s, a, \xi_{\geq t})$	Q and V functions for policy π starting from s where exogenous inputs are given by $\xi_{\geq t}$ (see Lemma 1)
$\mathbb{E}[\cdot]$	Empirical expectation taken where ξ is sampled uniformly from \mathcal{D}
$\bar{\pi}^*$	Policy obtained by ERM, i.e. solving $\text{argmax}_{\pi \in \Pi} \mathbb{E}[V_1^\pi(s_0, \xi)]$.
$\bar{\mathcal{P}}_\Xi, \bar{Q}_t, \bar{V}_t, \bar{\pi}$	Estimated exogenous distribution, Q_t^*, V_t^* estimates using the prediction, and the resulting policy
Hindsight Planner	
$Q_t^\dagger(s, a, \xi_{\geq t})$	$r(s, a, \xi_t) + \text{HINDSIGHT}(t+1, \xi_{>t}, f(s, a, \xi_t))$
$V_t^\dagger(s, \xi_{\geq t})$	$\text{HINDSIGHT}(t, \xi_{\geq t}, s)$
$Q_t^\dagger(s, a), V_t^\dagger(s, a)$	Expectations of $Q_t^\dagger(s, a, \xi_{\geq t})$ and $V_t^\dagger(s, \xi_{\geq t})$ over $\xi_{\geq t}$
π^\dagger	Greedy policy with respect to Q^\dagger
$\Delta_t^\dagger(s)$	Hindsight bias for state s at time step t (see Equation (9))
Δ	Absolute bound on $\Delta_t^\dagger(s)$
$\bar{\mathcal{P}}_\Xi$	Empirical distribution over ξ from \mathcal{D}
$\bar{\pi}^\dagger$	Greedy policy with respect to \bar{Q}^\dagger where true expectation over \mathcal{P}_Ξ replaced with $\bar{\mathcal{P}}_\Xi$
$\bar{\Delta}_t^\dagger(s)$	Value of $\Delta_t^\dagger(s)$ where expectation over \mathcal{P}_Ξ replaced with $\bar{\mathcal{P}}_\Xi$
$\bar{\text{Pr}}_t^{\bar{\pi}^\dagger}$	State visitation distribution of $\bar{\pi}$ at time step t with exogenous dynamics $\bar{\mathcal{P}}_\Xi$

Table 2: List of common notation

B Detailed Related Work

There is an extensive literature on reinforcement learning and its connection to tasks in operations management; below, we highlight the work which is closest to ours, but for more extensive references, see [71, 3, 59] for RL, [61] for background on MDPs, and [18, 66] for background on multi-armed bandits.

Information Relaxation for MDP Control: Information relaxation as an approach for calculating performance bounds on the optimal Q^* function has been developed recently using rich connections to convex duality [75, 17, 8, 15, 47]. As discussed in the main paper, for general problems, using hindsight planning oracles as in Assumption 2 creates estimates for the Q^* value which are overly optimistic of their true value. These differences can be rectified by introducing a control variate, coined *information penalties*, to penalize the planner’s access to future information that a truly non-anticipatory policy would not have. The goal is to construct penalties which ensure that the estimates of Q^* are truly consistent for the underlying value. This work has been developed explicitly in the context of infinite horizon MDPs [15] where constructions are given for penalty functions as a function of the future randomness of the ξ process. Moreover, concrete algorithmic implementations using hindsight planners and information penalties has been developed in the tabular setting with no finite sample guarantees [30]. In practice, the construction of these penalties is unclear. Our work differs by foregoing consistency of the estimates to instead focus on showing that in problem domains of interest, the policy which is greedy with respect to the hindsight planner is indeed consistent.

Policy Based Methods with Control Variates: Recent work has developed black box tools to modify policy gradient algorithms with control variates that depend on the exogenous trace. Recall that a typical policy-based algorithm uses either on-policy data (or off-policy with re-weighted importance sampling strategies), and estimates the gradient in the return via

$$\nabla R_{\pi_\theta} = \mathbb{E}_{S \sim \text{Pr}_t^{\pi_\theta}, A \sim \pi_\theta} [\nabla \log \pi_\theta(A | S) \hat{Q}^{\pi_\theta}(S, A)].$$

From here, most methods subtract off an appropriate baseline (commonly taken to be an estimate of the value function) as a form of Rao-Blackwellization to reduce the variance of the estimator while incurring no additional bias. In particular, for any function $b : \mathcal{S} \rightarrow \mathbb{R}$ we can instead take

$$\nabla R_{\pi_\theta} = \mathbb{E}_{S \sim \text{Pr}_t^{\pi_\theta}, A \sim \pi_\theta} [\nabla \log \pi_\theta(A | S) (Q_{\pi_\theta}(S, A) - b(S))]$$

while remaining unbiased. However, due to the exogenous input structure on the MDP any function $b : \mathcal{S} \times \Xi^T \rightarrow \mathbb{R}$ also results in an unbiased gradient. Through this, the existing literature has taken different approaches for constructing these *input driven baselines*. In [55] they consider directly using a baseline of the form $b(s, \xi)$. As an architecture to learn a network representation of this baseline the authors propose either using a multi-value network or meta learning. In [56] they consider using future conditional value estimates for the policy gradient baseline. In particular, they use Ψ_t as a new statistic to calculate new information from the rest of the trajectory and learn value functions which are conditioned on the additional hindsight information contained in Ψ_t . They provide a family of estimators, but do not specify which form of Ψ_t to use in generating an algorithm.

Recurrent Neural Network Policy Design: A related line of work modifies black box policy gradient methods by using a recurrent neural network (RNN) explicitly in policy design. In [74] they augment the state space to include ξ while simultaneously limiting information flow in the neural network to ensure that the algorithm is not overly relying on this privileged information. This approach, named *policy gradients incorporating the future*, is easy to implement as it just

augments the network using an LSTM and adds a new loss term to account for the information bottleneck.

Learning to Search: The Exo-MDP model is closely related to the learning-to-search model. Expert iteration [7] separates planning and generalization when learning to search, and provides an alternative approach to implement the HINDSIGHT oracle. Retrospective imitation [67] faces a similar challenge as us: a given ξ defines a fixed search space and we seek search policies that generalize across $\mathcal{P}_{\Xi}(\xi)$. However, retrospective imitation reduces to realizable imitation problems because the learner witnesses ξ beforehand whereas in Exo-MDPs, $\xi_{\geq t}$ is privileged information and imitating HINDSIGHT is typically unrealizable. Asymmetric Imitation Learning [78] studies problems when imitating an expert with privileged information but essentially use RNN policies to ameliorate unrealizability.

RL for OR: In our work we primarily consider simulations on dynamic Virtual Machine (VM) scheduling. On the theoretical side, variants of greedy algorithms have been usually proposed to solve the dynamic VM scheduling problems with competitive ratio analysis. In [69] they assume the VM creation requests can be modeled as a Poisson process with lifetimes as an exponential distribution and show the greedy algorithm achieves the asymptotically optimal policy. In [49] they develop a hybrid FIRSTFIT algorithm with an improvement on the competitive ratio. On the more practical side using deep reinforcement learning techniques, in [53] they develop a DeepRM system which can pack tasks with multiple resource demands via a policy gradient method. They also built a job scheduler named DECIMA by modifying actor critic algorithms with input driven baselines [54]. In [82] they solved the heterogeneous scheduling problem with deep Q learning. Lastly, in [64] they developed SchedRL, a modification of Deep Q Learning with reward shaping to develop a VM scheduling policy. All of these algorithms modify existing Sim2Real RL algorithms and show empirical gains on variations of the VM scheduling problem. Our work differs from two perspectives: 1) we consider using hindsight planning explicitly during training time, 2) our algorithms directly modify existing Sim2Real RL algorithms for these input driven MDP problems.

We also note that reinforcement learning has also been applied in other systems applications including ride-sharing systems [33], stochastic queueing networks [25], power grid systems [19], jitter buffers [31], and inventory control [42], by applying existing deep RL algorithms to these problem domains.

RL for Combinatorial Optimization: A crucial assumption underpinning our algorithmic framework is the implementation of hindsight planners as in Assumption 2. Our framework is well motivated for problems where hindsight planning is efficient, building on the existing optimization literature on solving planning problems [23, 11]. However, in general these problems as a function of a fixed exogenous input trace can be written as combinatorial optimization problems. While we consider using hindsight planners for RL problems, a dual lens is using machine learning techniques for combinatorial optimization, as has been explored in recent years [77, 10, 21]. In particular, in [77] they designed a new network architecture and trained using supervised learning for traveling salesman problems. Similarly in [44] they solve variants of online bin packing problems using policy gradient algorithms. In [72] they design novel heuristic branch and bound algorithms using machine learning for integer programming optimization.

Input Driven Models: Input driven MDPs, as highlighted in Section 3 was first outlined in [59]. They characterize sequential decision making problems as an evolution of *decision, information, decision, information* sequence represented mathematically as the sequence $(s_1, a_1, \xi_1, s_2, a_2, \xi_2, \dots, s_T)$. Here, the state variable s_t is written explicitly to capture the information available to the decision maker to make a decision a_t , followed by the information we learn after making a decision, i.e. the exogenous information ξ_t . Similar models have been outlined in [55, 26, 29].

Existing literature has coined many names for these models, including “Input Driven MDPs” [55]

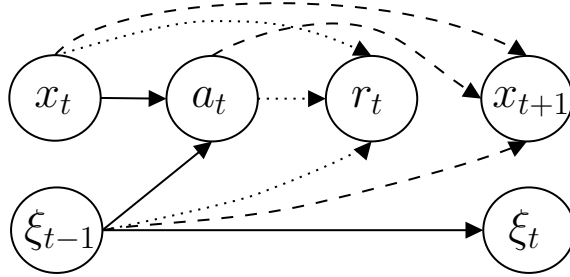


Figure 2: Causal diagram for an input driven MDP where $k = 1$. Here the dotted line indicates the influence of (x_t, a_t, ξ_t) on the immediate reward r_t via $r(x_t, a_t, \xi_t)$ and the dashed line on the transition evolution as $x_{t+1} = f(s_t, a_t, \xi_t)$. The key facet to notice is the lack of influence on the ξ process from the current endogenous state x_t and action a_t .

and “MDPs with Exogenous Variables” [26]. Our model *subsumes and generalizes* both of these in the literature. In particular, in contrast to “input driven MDPs” our model allows arbitrary correlation structure on the exogenous inputs (instead of assuming they are i.i.d.). Contrary to “MDPs with Exogenous Variables” we allow reward functions which depend *arbitrarily* on the state variables and exogenous inputs. These more directly mimic problems of interest in the operations management community (and is discussed further in Appendix C).

C MDPs with Exogenous Inputs

In this section we further discuss the definition of MDPs with exogenous inputs, highlight some examples in the operations management literature, and give implementations for the hindsight planner from Assumption 2.

C.1 Generality of MDPs with Exogenous Inputs

As highlighted in Section 3 we consider the finite horizon reinforcement learning setting where an agent is interacting with a Markov Decision Process (MDP) [61]. The underlying MDP is given by a five-tuple $(\mathcal{S}, \mathcal{A}, T, p, R, s_1)$ where T is the horizon, $(\mathcal{S}, \mathcal{A})$ denotes the set of states and actions, R is the reward distribution, p the distribution governing the transitions of the system, and s_1 is the given starting state.

Definition 2. *In an MDP with Exogenous Inputs we let $\xi = (\xi_1, \dots, \xi_T)$ be a trace of exogenous inputs with each ξ_t supported on the set Ξ . We assume that ξ is sampled according to an unknown distribution \mathcal{P}_Ξ . The agent has access to an endogenous or system state $x \in \mathcal{X}$. With this, the dynamics and rewards of the Markov decision process evolve where at time t , the agent selects their action $a_t \in \mathcal{A}$ based solely on $s_t = (x_t, \xi_{<t})$. After, the endogenous state evolves according to $x_{t+1} = f(s_t, a_t, \xi_t)$, and the reward earned is $r(s_t, a_t, \xi_t)$, and ξ_t is observed. We assume that f and r are known by the principal in advance.*

Note that this imposes that the state space for the underlying MDP can be written as $\mathcal{S} = \mathcal{X} \times \Xi^T$ where the first component corresponds to the endogenous state and the second to the exogenous input trace observed so far. The distributional assumption additionally imposes that:

$$r(s_t, a) = \int_{\Xi} r(s_t, a, \xi_t) d\mathcal{P}_\Xi(\xi_t | \xi_{<t})$$

$$p(x_{t+1}, \boldsymbol{\xi}_{\leq t} \mid s_t, a) = \mathbb{1}_{[x_{t+1}=f(s_t, a_t, \xi_t)]} \mathcal{P}_{\Xi}(\xi_t \mid \boldsymbol{\xi}_{<t})$$

We use the shorthand s_t to refer to $(x_t, \boldsymbol{\xi}_{<t})$.

As written, the distribution \mathcal{P}_{Ξ} can be arbitrarily correlated across time. We can relax this setting to assume that $\boldsymbol{\xi}$ evolves according to a k -Markov chain. More formally, that at each step t , $\xi_t \mid (\xi_{t-k}, \xi_{t-k+1}, \dots, \xi_{t-1})$ is conditionally independent of $(\xi_1, \dots, \xi_{t-k-1})$. This allows the state space to be represented as $\mathcal{S} = \mathcal{X} \times \Xi^k$.

For more intuition, consider the model under various values of k :

- **Case $k = T$:** Here we assume that $\boldsymbol{\xi}$ is an arbitrarily correlated process and $\mathcal{S} = \mathcal{X} \times \Xi^T$ so that $s_t = (x_t, \boldsymbol{\xi}_{<t})$.
- **Case $k = 1$:** Here we assume that $\boldsymbol{\xi}$ process evolves according to a 1-Markov chain. The state space factorizes as $\mathcal{X} \times \Xi$ where \mathcal{X} is the endogenous space and Ξ is the exogenous space. The current state is $s_t = (x_t, \xi_{t-1})$, and the state updates to $(f(s_t, a_t, \xi_t), \xi_t)$ where ξ_t is drawn from the conditional distribution given ξ_{t-1} . A representation of the causal diagram under this setting is in Figure 2. This setting has been considered previously in the literature in [26, 55] as an *input driven MDP*.
- **Case $k = 0$:** Here we have that $\mathcal{S} = \mathcal{X}$. After taking an action based a_t based solely on x_t we transition to $x_{t+1} = f(x_t, a_t, \xi_t)$ with ξ_t sampled independently from an unknown distribution \mathcal{P}_{Ξ}^T . The previous variable ξ_t can be either observed or unobserved. We will see that this setting is equivalent to the typical MDP model with different assumptions on the underlying dynamics and rewards.

The dataset \mathcal{D} contains a series of N traces sampled independently according to \mathcal{P}_{Ξ} as $\mathcal{D} = \{\boldsymbol{\xi}^1, \dots, \boldsymbol{\xi}^N\}$ where each $\boldsymbol{\xi}^i = \{\xi_1^i, \dots, \xi_T^i\}$. When f is invertible onto Ξ we can instead consider access to a logged dataset of N trajectories under an arbitrary behavioural policy of the form $(x_t, a_t, r_t, x_{t+1})_{t=1}^T$. With this we can reconstruct ξ_t since x_{t+1} is a unique function of ξ_t for some $\xi_t \in \Xi$.

We focus briefly on the case when $k = 0$, showing that our model is essentially equivalent to the typical model in RL with only differences on the underlying assumptions. The typical assumptions in RL involve that $s_{t+1} \sim p(\cdot \mid s_t, a_t)$ where the underlying distribution p is unknown. This can be written equivalently as $s_{t+1} = f(s_t, a_t, \xi_t)$ where ξ_t is sampled uniformly in $[0, 1]$ and the underlying function f is unknown. As such, typically in RL we consider:

- Unknown structure of the dynamics and rewards (i.e. unknown f and r)
- Known distribution on the underlying exogenous inputs where each ξ_t is uniform over $[0, 1]$
- Access to a logged dataset of (s_t, a_t, r_t, s_{t+1}) pairs

In our model we instead assume:

- Known structure of the dynamics and rewards (i.e. known f and r)
- Unknown distribution on the exogenous inputs \mathcal{P}_{Ξ}
- Access to a dataset of exogenous traces ξ_1, \dots, ξ_T

These types of assumptions (where the *form* of the randomness is known but the true underlying distribution is unknown) is common in the graphon literature [12, 50]. In the following lemma we show that these two models are equivalent, in that any MDP can be written as an MDP with exogenous inputs and $k = 0$.

Lemma 8. Any MDP of the form $(\mathcal{S}, \mathcal{A}, T, p, R, s_1)$ where the distribution on p and R are unknown has an equivalent exogenous input form with $k = 0$, and vice-versa.

Proof. Without loss of generality we will assume that both Ξ and \mathcal{S} are either discrete or one dimensional (where higher dimensions follow via the same philosophy).

Exogenous Inputs \rightarrow **RL:** Suppose that $s_{t+1} = f(s_t, a_t, \xi_t)$ where ξ_t is sampled from \mathcal{P}_Ξ and f is known.

We can write this of the form where f is unknown and \mathcal{P}_Ξ is known by setting $\tilde{\xi}_t \sim U[0, 1]$ and $\tilde{f}(s_t, a_t, \tilde{\xi}_t) = f(s_t, a_t, \mathcal{P}_\Xi^{-1}(\tilde{\xi}_t))$. Here the form of \tilde{f} is unknown as we cannot evaluate \mathcal{P}_Ξ^{-1} , but the distribution on the underlying randomness $\tilde{\xi}$ is known.

RL \rightarrow **Exogenous Inputs:** Suppose that $s_{t+1} \sim p(\cdot | s_t, a_t)$ where the distribution is unknown. We can write this as $s_{t+1} = f(s_t, a_t, \xi_t)$ with a known f and unknown distribution \mathcal{P}_Ξ as follows.

First set $\Xi = \Delta(\mathcal{S})^{\mathcal{S} \times \mathcal{A}} \times [0, 1]$. Given any $\xi \in \Xi$ we define the transition kernel $f(s_t, a_t, \xi)$ as follows:

- Set $\tilde{p} \in \Delta(\mathcal{S})$ to be the component of ξ indexed via s_t, a_t
- Letting z be the last component of ξ , set $s_{t+1} = \tilde{p}^{-1}(z)$.

The distribution over Ξ is then defined as an indicator variable over the first $\mathcal{S} \times \mathcal{A}$ components indicating the true unknown distribution p , and the last component over $[0, 1]$ being Uniform $[0, 1]$. \square

C.2 Examples of Input Driven MDPs

We now give several examples of input driven MDPs alongside with their exogenous decomposition of the transition distribution. We also highlight the underlying Markovian assumption on the exogenous inputs ξ .

C.2.1 Ambulance Routing via Metrical Task Systems ($k = 0$)

Consider an ambulance operator who sequentially decides locations to station k ambulances in order to preempt service requests [65, 14]. This ambulance routing model is also referred to as metrical task system or k -servers in the theoretical computer science literature [2, 13, 22, 52].

The operator has access to a set of locations \mathcal{X} and patient arrival locations $\Xi = \mathcal{X}$. At every round t , the operator decides on locations $a \in \mathcal{X}^k$ to station each of the k ambulances, paying a transportation cost. Afterwards, the closest ambulance i travels from location a_i to the exogenous arrival located at ξ drawn from \mathcal{P}_Ξ . The reward function for the problem is as follows:

$$r(x, a, \xi) = \alpha \mathcal{D}(x, a) + (1 - \alpha) \min_i \mathcal{D}(a_i, \xi)$$

where $\alpha \in [0, 1]$ serves as a tuning parameter for the costs of moving the ambulances to the desired location a , $1 - \alpha$ is the increased cost of traveling to service the patient, and \mathcal{D} is an arbitrary function (typically taken to be a metric). The state transition function is $x' = f(x, a, \xi)$ where $x'_i = a_i$ for all $i \neq \operatorname{argmin}_i \mathcal{D}(a_i, \xi)$ with $x'_i = \xi$ for that index.

C.2.2 Inventory Control with Lead Times and Lost Sales ($k = 0$)

This models a single product stochastic inventory control problem with lost sales and lead times [4, 36, 80, 32]. In the beginning of every time step t , the inventory manager observes the current

inventory level Inv_t and L previous unfulfilled orders in the pipeline, denoted o_L, \dots, o_1 for a product. L denotes the lead time or delay in the number of time steps between placing an order and receiving it. The next inventory is obtained as follows. First, o_1 arrives and the on-hand inventory rises to $I_t = \text{Inv}_t + o_1$. Then, an exogenous demand ξ is drawn independently from the unknown demand distribution \mathcal{P}_Ξ . The cost to the inventory manager is

$$h(I_t - \xi)^+ + p(\xi - I_t)^+$$

where h is the holding cost for remaining inventory and p is the lost sales penalty. The on-hand inventory then finishes at level $(I_t - \xi)^+$.

This can be formulated as an input driven MDP by letting $\mathcal{X} = [n]^{L+1}$ denote the current inventory level and previous orders, $\Xi = [n]$ as the exogenous demand, and $\mathcal{A} = [n]$ for the amount to order where n is some maximum order amount. The reward function is highlighted above, and the state transition updates as $x' = f(x_t, a_t, \xi)$ where $\text{Inv}_{t+1} = (\text{Inv}_t + o_1 - \xi)^+$, $o_k = o_{k-1}$ for all $1 < k < L$ and $o_L = a$. This model can also be expanded to include multiple suppliers with different lead times.

C.2.3 Online Stochastic Bin Packing ($k = 1$)

Here we consider a typical online stochastic bin packing model [40, 35, 58] where a principal has access to an infinite supply of bins with maximum bin size B . Items u_t arrive over a sequence of rounds $t = 1, \dots, T$ where each $u_t \in [B]$ denotes the item size. At every time step, the principal decides on a bin to allocate the item to, either allocating it to a previously opened bin or creating a new bin. The goal is to allocate all of the items using the smallest number of bins.

This can be modeled in the framework as follows. Here we let $\mathcal{X} = \mathbb{R}^B$, $\Xi = [B]$ and $\mathcal{A} = [B]$. Each vector $x \in \mathcal{X}$ has components x_1, \dots, x_B as the current number of bins opened with current utilization of one up to B , with Ξ corresponding to the current item arrival's size. Hence the state space is $\mathcal{S} = \mathcal{X} \times \Xi$ where $s_t = (x_t, \xi_{t-1})$ corresponds to the current bin capacity and current item arrival. Actions $a \in \mathcal{A}$ correspond to either 0, for opening up a new bin, or $1, \dots, B$ to be adding the current item to an existing bin with current utilization one up to B . The reward is:

$$r(x_t, \xi_{t-1}, a, \xi_t) = \begin{cases} -1 & a = 0 \\ 0 & a > 0, s_a > 0, \text{ and } a + \xi_{t-1} \leq B \\ -100 & \text{otherwise} \end{cases}$$

where -1 corresponds to the cost for opening a new bin, and the condition on zero reward verifies whether or not there is currently an open bin at level a and the action is feasible (i.e. allocating the current item to the bin at size a is smaller than the maximum bin capacity).

The transition distribution is updated similarly. Let ξ_t be drawn from the conditional distribution given ξ_{t-1} . If $a = 0$ then $x' = x$ except $x'_{\xi_{t-1}}$ is incremented by one (for opening up a new bin at the level of the size of the current item). If $a > 0$ and the action is feasible (i.e. $s_a > 0$ and $a + \xi_{t-1} \leq B$) then $x' = x$ with $x'_{a+\xi_{t-1}}$ incremented by one and x'_a decreased by one.

We note again that this model can be extended to include different reward functions, multiple dimensions of item arrivals, and departures, similar to the Virtual Machine allocation scenario.

C.2.4 Virtual Machine Allocation ($k = T$)

The Cloud has modified the way that users are able access computing resources [63, 46, 24, 45, 41]. Cloud service providers allow customers easy access to resources while simultaneously applying

efficient management techniques in order to optimize their return. One of the most critical components is the Virtual Machine (VM) allocator, which assigns VM request to the physical hardware (henceforth referred to as PMs). The important issue is how to allocate physical resources to service each VM efficiently by eliminating fragmentation, performance impact and delays, and allocation failures.

These VM allocation models can be thought of as a multi-dimensional variant of bin-packing with an additional component of arrival and departures. The typical VM scheduling scenarios models users requesting resources over time, where each request contains the required CPU and memory uses, and its lifetime. The allocator then decides which available physical machine to allocate the virtual machine to. To limit notational overload, we provide a high level view of the Virtual Machine allocation scenario here, and defer concrete discussion and notation when discussing the planning oracle required for solving.

In this set-up the current system state of the model is measured by the physical resources available for each PM, including the physical cores and memory available. Over time,

- Coming VM requests ask for a certain amount of resources (CPU and memory requirements) and their lifetime. Resource requirements are varied based on the different VM requests.
- Based on the action selected by the algorithm, the VM will be allocated to and be created in a specified PM as long as that PM’s remaining resources are enough.
- After a period of execution, the VM completes its tasks. The simulator will then release the resources allocated to this VM and deallocate this VM from the PM.

At a high level, these problems can be modeled as an MDP with exogenous inputs where the exogenous space Ξ contains the space of possible VM requests (along with their lifetime, memory, and CPU requirements). The endogenous space \mathcal{X} measures the current capacity of each physical machine on the server, and action space \mathcal{A} for allocation decisions for the current VM request to a given PM. More details on the concrete experimental set-up will be in Appendix E. We also note that the VM arrival process in practice is highly correlated so this fits under the model where $k = T$ [41].

D Hindsight Planners

Here we outline the feasibility of Assumption 2 in many operations tasks. Planning problems induced by online knapsack problems as a function of a deterministic input sequence ξ can be solved via their induced linear relaxation in pseudo-polynomial time (as the constraint polytope is a polymatroid). Other problems, such as inventory control with lead times have planning problems where a simple greedy control policy is optimal. More generally, Assumption 2 requires us to solve large-scale combinatorial optimization problems. However, we note that all of these computations are done *offline* and so the computational burden is not required at run-time. Moreover, it is easy to incorporate existing heuristics from the optimization literature for efficient solutions to these problems, including linear programming or fluid relaxations [23]. This appeals to our HINDSIGHT LEARNING algorithms only relying on the objective value of the planner, instead of the actual sequence of actions.

D.1 Bin Packing

We give the integer programming representation of the optimal open loop control for Bin Packing as follows. Consider a state x with components x_1, \dots, x_B as the current number of bins opened with

a utilization of 1 up to B and a sequence of items with sizes $\xi = (u_1, \dots, u_T)$. Given (x_1, \dots, x_B) we pre-process this list to a vector of length $\sum_i s_i$ where each component corresponds to the current utilization of any bin. For example, if $B = 3$ and $x = (1, 0, 2)$ then we make a list containing $\alpha = (1, 3, 3)$ for two bins with a utilization of three and one bin with a total utilization of one. Since the total number of bins required will be $\sum_i x_i + T$ we use the variables y_b for $b \in [\sum_i x_i + T]$ to denote an indicator of whether or not bin y_b is currently utilized. We also use variables $z_{v,b}$ to denote whether item $v \in [T]$ is assigned to bin b . Similarly, denote α_b as the current utilization of a bin b . The optimization program can then be written as follows:

$$\begin{aligned} \max_{z,y} & - \sum_b y_b \\ \text{s.t.} & \sum_b z_{v,b} = 1 \text{ for all } v \in [T] \\ & \sum_v z_{v,b} + \alpha_b \leq B y_b \text{ for all } b \\ & y_b = 1 \text{ for any } b \text{ with } \alpha_b > 0 \end{aligned}$$

The objective corresponds to minimizing the number of utilized bins. The first constraint ensures that each item is assigned to a bin. The second constraint enforces capacity constraints for each bin, and the last constraint ensures that bins are marked as used if they have current utilization on them (i.e. $\alpha_b > 0$). An implementation of this simulator and the planning oracle is provided in the attached code base.

D.2 Inventory Control

In inventory control, given knowledge of the exact sequence of demands $\xi = (d_1, \dots, d_T)$, the optimal open loop control policy is trivial to write down. Indeed, setting:

$$a_t = \begin{cases} d_{t+L} & t \leq T - L \\ 0 & \text{otherwise} \end{cases}$$

is clearly the optimal policy. This is as, for any $t \leq T - L$ we ensure the current on-hand inventory is exactly equal to that period's demands. For the last L periods we order nothing in order to minimize the accumulated purchase costs for inventory which will be ordered and cannot be sold. An implementation of this simulator and the planning oracle is provided in the attached code base.

D.3 Virtual Machine Allocation

The planning oracle for the VM allocation problem can be formulated as a large-scale mixed integer linear program. In this section we discuss approaches which utilize this fact in developing an oracle for the hindsight planning problem.

Use $\Xi = V$ to denote the set of VM requests and P as the set of physical machines. We use the following constants which depend on the current inventory of virtual and physical machines contained in the current state s_t , including:

- $\alpha_{t,p}$ for the remaining CPU cores for physical machine p at event t
- $\beta_{t,p}$ for the remaining memory for physical machine p at event t
- CPU-CAP $_p$ and MEM-CAP $_p$ the CPU and memory capacity of physical machine $p \in P$

- $LIFETIME_v$, $CORE_v$, MEM_v as the lifetime, cores, and memory utilization of VM $v \in V$
- $\eta_{v,t}$ an indicator that the VM v is active at time t (i.e. $\eta_{v,t}$ is equal to one for any time starting from the time the VM v arrives until the end of its lifetime)

With this we introduce variables $x_{v,p}$ for each virtual machine v and physical machine p to indicate the assignments. We also use variables $y_{t,p}$ which encode whether physical machine p has a VM assigned to it at time step t .

We start by considering the various constraints in the problem:

- **Assignment Constraint** (Equation (14)): For every v we need $\sum_p x_{v,p} = 1$ indicating that each virtual machine is assigned to a physical machine.
- **CPU Capacity Constraint** (Equation (15)): For every p and t we need $\alpha_{p,t} + \sum_v CORE_v \eta_{v,t} x_{v,p} \leq CPU-CAP_p$ to ensure CPU usage capacity constraints are satisfied.
- **Memory Capacity Constraint** (Equation (16)): For every p and t we need $\beta_{p,t} + \sum_v MEM_v \eta_{v,t} x_{v,p} \leq MEM-CAP_p$ to ensure memory capacity constraints are satisfied.

We also need additional constraints which encode the $y_{t,p}$ variable as follows:

- **PM Historical Utilization** (Equation (17)): $y_{t,p} \geq 1$ for all p and t if $\alpha_{t,p} > 0$
- **PM VM Utilization** (Equation (18)): $x_{v,p} \eta_{v,t} \leq y_{t,p}$ for all v and p
- **PM OR Constraint** (Equation (19)): $\sum_v x_{v,p} \eta_{v,t} + \mathbb{1}_{[\alpha_{t,p} > 0]} \geq y_{t,p}$ for all t and p .

These constraints essentially encode that $y_{t,p}$ is an indicator for whether y has a VM assigned to it from ξ (in the second bullet), or has historical allocations on it (for when $\alpha_{t,p} > 0$).

We note that there always exists a feasible solution since we are in an over provisioned regime where we have capacity to service every VM request.

Lastly, the objective function (Equation (13)) for the packing density can be formulated via:

$$- \sum_t \frac{\sum_p y_{t,p} CPU-CAP_p}{\sum_p \alpha_{t,p} + \sum_v CORE_v}$$

The numerator corresponds to the total CPU capacity of all physical machines which are in use. The denominator corresponds to the total utilization (both from the VMs currently in service and the VMs arriving over the time horizon). This then encodes the inverse of the core packing density, as described earlier.

The full integer program is now summarized below:

$$\max_{x,y} - \sum_{t \in [T]} \frac{\sum_{p \in P} y_{t,p} CPU-CAP_p}{\sum_{p \in P} \alpha_{t,p} + \sum_{v \in V} CORE_v} \quad (13)$$

$$\text{s.t. } \sum_{p \in P} x_{v,p} = 1 \quad \forall v \in V \quad (14)$$

$$\alpha_{p,t} + \sum_{v \in V} CORE_v \eta_{v,t} x_{v,p} \leq CPU-CAP_p \quad \forall t \in [T], p \in P \quad (15)$$

$$\beta_{p,t} + \sum_{v \in V} MEM_v \eta_{v,t} x_{v,p} \leq MEM-CAP_p \quad \forall t \in [T], p \in P \quad (16)$$

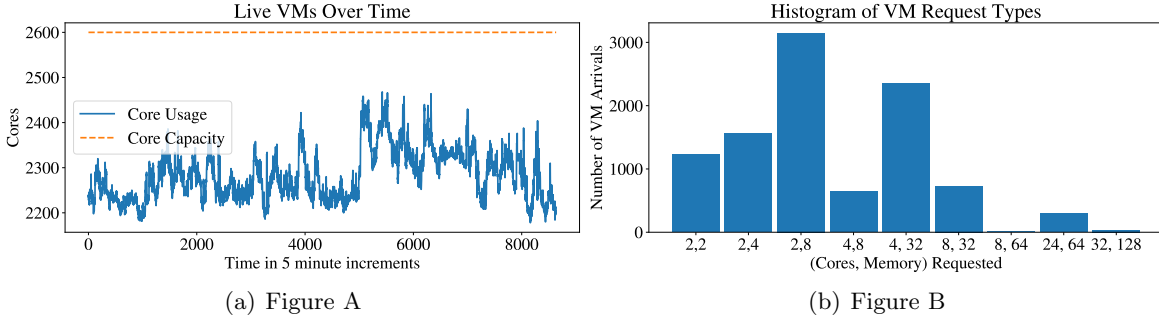


Figure 3: Sample of a thirty-day roll-out of the 2019 workload from the Microsoft Azure traces. In Figure 3(b) we show a histogram of the various VM types and their corresponding cores and memory resources requested. In Figure 3(a) we plot the used cores over time on the observed trace, along with the capacity of the cluster.

$$y_{t,p} \geq \mathbb{1}_{[\alpha_{t,p} > 0]} \quad \forall t \in [T], p \in P \quad (17)$$

$$x_{v,p} \eta_{v,t} \leq y_{t,p} \quad \forall v \in V, t \in [T], p \in P \quad (18)$$

$$\sum_{v \in V} x_{v,p} \eta_{v,t} + \mathbb{1}_{[\alpha_{t,p} > 0]} \geq y_{t,p} \quad \forall t \in [T], p \in P \quad (19)$$

An implementation of this program along with heuristic computational improvements via warm-starting and initialization methods are provided in the attached code base.

E Simulation Details

In this section we provide full details on the simulations conducted, including a formal description of virtual machine allocation scenarios along with its fidelity to the true Microsoft Azure system, training implementations, hyperparameter tuning results, and a description of the heuristic algorithms compared.

E.1 Virtual Machine Allocation Simulations

Cloud computing has revolutionized the way that computing resources are consumed. These providers give end-users easy access to state-of-the-art resources. One of the most crucial components to cloud computing providers is the Virtual Machine (VM) allocator, which assigns specific VM requests to physical hardware. Improper placement of VM requests to physical machines (henceforth referred to as PMs) can cause performance impact, service delays, and create allocation failures.

The Microsoft Azure system consists of millions of physical machines spanning more than a hundred countries, offering more than five hundred different VM types (see Figure 3(b)). The VMs serve as the primary units of resource allocation in these models. We focus on designing allocation policies at the *cluster* level, which are a homogeneous set of physical machines with the same memory and CPU cores capacity.

The cluster-specific allocator is tasked with the following:

- Coming VM requests ask for a certain amount of resources (CPU and memory requirements) along with their lifetime. Resource requirements are varied based on the different VM requests.

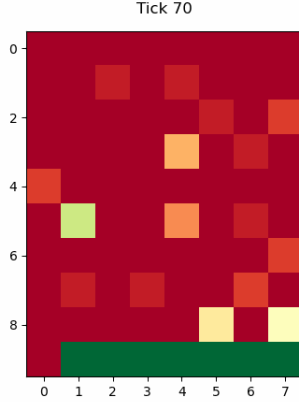


Figure 4: Packing density for the Best Fit policy at one time-step. Each square corresponds to a specific PM and the colour corresponds to what portion of that PM’s capacity is currently utilized. Red corresponds to fully used, green is completely empty. The packing density ignores the empty (or green) PMs on the bottom and counts the cumulative utilization ratio for the remaining PMs.

- Based on the action selected by the allocator policy, the VM will be allocated to and be created in a specified PM as long as that PM’s remaining resources are enough.
- After a period of execution, the VM completes its tasks. The simulator will then release the resources allocated to this VM and de-allocate this VM from the PM.

We use **MARO**, an open source package for multi-agent reinforcement learning in operations research tasks as a simulator for the VM allocator [46]. In this scenario the VM requests are uniformly sampled from 2019 historical Microsoft Azure workloads [24]. We focus on a 30 day reading of the 2019 utilization of the Azure public systems on the JP1 cluster of the **Asia-Northeast-1** availability zone. See Figure 3(a) to highlight the demand workflow for the cluster considered in 2019.

By default, **MARO** provides reward metrics that can be used when specifying the objective of the algorithm. The metrics provided include income, energy consumption, profit, number of successful and failed allocations, latency, and total number of overloaded physical machines. However, typical cloud computing systems run in an *over-provisioned* regime where the capacity of the physical machines is larger than the demand in order to ensure quality of service to its customers. As a result, any reasonable algorithm has no failed allocations. Hence, any reasonable algorithm also has identical values for income, energy consumption, profit, etc.

For the reward function we instead consider $r(s, a, \xi) = -100 * \text{Failed-Allocation} - 1 / \text{Packing Density}$. The first component, one hundred times the number of failed allocations, helps to penalize the algorithms in training to ensure valid assignments for all of the VM requests. The second component corresponds to the **Packing-Density**, computed via:

$$\text{Packing-Density} = \frac{\sum_{v \in VM} \text{Cores Usage}_v}{\sum_{p \in PM} \mathbb{1}_{[p \text{ is utilized}]} \text{Capacity}_p}$$

The numerator here is the total cumulative cores used for all of the VMs currently assigned on the system. The denominator is the total capacity of all physical machines which are currently utilized (i.e. have a VM assigned and currently running). The reason for picking this reward (and the inverse of it) is that:

- It allows for an easily expressible linear programming formulation (see Appendix D.3).
- For any two policies which allocate all virtual machines, packing density serves as a criteria to differentiate the policies. An algorithm which has large packing density equivalently uses the physical machines efficiently so that unused PMs can be re-purposed, reassigned, or potentially turned off.
- It serves as a proxy to ensure that the virtual machines are packed in as minimal number of physical machines possible. This allows the allocator to be robust to hardware failures, where entire physical machines are potentially rendered unusable.

See Figure 4 for an illustration.

E.2 Simulator Fidelity

Our training procedure requires a faithful simulator of Virtual Machine allocation focused at a cluster level to validate our experimental results. We found that the **MARO** simulator captures all first-order effects of cloud computing environments specifically at the cluster level. However, there are several effects not included in the simulations:

- When a virtual machine arrives to the system, they request a *maximum* amount of CPU and memory capacity that they can use. However, over time, any given VM request might only use a fraction of their requested resources. Current cloud computing systems use an *over-subscription* model where the requested memory and CPU cores for the VMs assigned to a PM can surpass its capacity. However, when the total realized demand surpasses the PMs capacity, all of the VMs assigned to that system are failed and migrated to a different PM. In contrast, **MARO** assumes that each VM uses exactly its requested cores and memory over time, hence eliminating the need to model over-subscription on the cluster level.
- Typical systems involve live migration where virtual machines can be moved between physical machines without disrupting the VM request. This is used in order to eliminate stranding which occurs when a physical machine has only a few long-running virtual machines allocated to it. However, such an operation is costly and requires a large amount of system overhead.
- Our neural networks explicitly use the VM’s lifetime as a feature in the state. However, in true cloud computing systems the lifetime is unknown. Only when a user decides to cancel a VM does the system have access to that information. As such, it is typically observed in the trace dataset but cannot be used in policy network design. We forgo this when modelling the policy as unlike the dynamics of VM request types, lifetimes for a VM are typically easy to model and these forecasts can be used as a replacement in the network representation [41].

We believe that **MARO** serves as a high fidelity simulator of the VM allocation problem at the cluster level while providing open source implementation for additional research experimentation.

E.3 Training Implementation Details

Algorithm 2 presents the pseudocode for our training procedure using **MARO**. We repeat the following process for five hundred roll-outs. Line 3 samples one-hour traces of VM requests from the 2019 historical Microsoft Azure dataset. Then, in line four and five, with fifteen actors in parallel we evaluate the current policy π_θ on the sampled VM request trace, adding the dataset of experience to the experience buffer. Lines 8-10 samples batches of size 256 where we update the policy and

Algorithm 2 Training Procedure in MARO

```
1: Input: number of roll-outs, number of actors, number of training iterations.
2: for each roll-out do
3:   For each actor, sample a one-hour trace of VM requests  $\xi^i$ 
4:   for each actor do
5:     Collect dataset of  $(s_t, a_t, \xi_t, r_t, s_{t+1})$  pairs under the current policy  $\pi_\theta$ 
6:   end for
7:   Add collected dataset to current experience buffer
8:   for each training iteration do
9:     Sub-sample batch from current collected dataset
10:    Update policy by gradient descent along the sampled batch
11:   end for
12: end for
```

algorithmic parameters θ by gradient descent on the loss function evaluated on the sampled batch. This process repeats for five thousand gradient steps.

We implemented the training framework using PyTorch [57] along with MARO [46], and all experiments were conducted using the Microsoft Azure ML platform. For hyperparameters and neural network architectures for the Sim2Real RL and HINDSIGHT LEARNING algorithms, see Appendix E.6.2. All experiments were run on the same compute hardware and took similar runtimes to finish. Runtime was dominated by the MARO simulator executing the roll-outs under the current policy versus the HINDSIGHT calls or the ML model updates. As such, each algorithm was essentially given the same computational budget.

E.4 Network Design and State Features

The state space of the VM allocation scenario is combinatorial as we need to include the CPU and memory utilization of each physical machine across time. To avoid this we use action-dependent features in the models. Once a VM request arrives we consider the set of PMs that are available and able to service this VM. Each (PM, VM) pair has associated state features including: the VM’s CPU and memory requirement with their lifetime, the PM’s CPU and memory capacity, and the historical utilization of the PM over the last three steps. The last component is a proxy for the historical utilization across all time to account for the currently assigned VMs.

These experiments are *semi-synthetic* as we use the VM’s lifetime as part of the state. This information is contained in the exogenous trace but typically not available at run-time. However, this feature could be replaced with a predictor as lifetimes are easier to predict than the sequence of VM resource requests [41].

For the actor and critic network representations in all algorithms we use a four layer neural network with (32, 16, 8) hidden dimensions, an output dimension of one (due to the action-dependent features), and LeakyReLU activation functions. For each of the algorithms we use the *RMSprop* optimization algorithm. We implemented the training framework using PyTorch [57] and MARO. All experiments were run on the same compute hardware and took similar runtimes to finish. Runtime was dominated by the MARO simulator executing the roll-outs, and the ML model updates and HINDSIGHT oracle calls were quicker.

To evaluate the trained policies we subdivided the 2019 historical Microsoft Azure dataset into a training and test portion. For evaluation we sampled fifty different one-day traces of VM requests from the held-out portion. For each of the different traces, we executed the policy in

parallel to a greedy **Best Fit** algorithm. Each deep learning algorithm was evaluated over five different random seed initializations and we tuned hyperparameters using grid search. All metrics are reported with respect to cumulative differences against the baseline **Best Fit** policy, alongside statistical significance tests. In Table 1 we evaluate the number of machines required to pack the jobs. Negative numbers correspond to fewer required PMs on average. Asterisks correspond to statistical significance computed with Welch’s t -test with $p = 0.05$.

E.5 Evaluation Details

To evaluate the trained policies we subdivided the 2019 historical Microsoft Azure dataset into a training and test portion. For evaluation we sampled fifty different one-day traces of VM requests from the held-out portion. For each of the different traces, we executed the policy in parallel to a greedy **Best Fit** algorithm. Each deep learning algorithm was evaluated over five different random seed initializations and we tuned hyperparameters using grid search. All metrics are reported with respect to cumulative differences against the baseline **Best Fit** policy, alongside a 95% confidence interval of the regret. In Table 4 we provide the performance metrics on the underlying rewards as well.

E.6 Benchmark Allocation Algorithms

We compared the performance of our HINDSIGHT LEARNING algorithms to Sim2Real RL algorithms and several natural heuristics in VM allocation.

E.6.1 Heuristic Algorithms

- **Random:** Picks a physical machine uniformly at random from the list of physical machines which have capacity to service the current VM request.
- **Round Robin:** Allocates to physical machines in a round-robin strategy by selecting a physical machine from the list of physical machines which have capacity to service the current VM request that was least recently used.
- **Best Fit:** This algorithm picks a physical machine based on a variety of metric types.
 - **Remaining Cores:** Picks a valid physical machine with minimum remaining cores
 - **Remaining Memory:** Picks a valid physical machine with minimum remaining memory
 - **Energy Consumption:** Picks the valid physical machine with maximum energy consumption
 - **Remaining Cores and Energy Consumption:** Picks a valid physical machine with minimum remaining cores, breaking ties via energy consumption

Similar heuristics to this are currently used in most large-scale cloud computing systems [41].

- **Bin Packing:** Selects a valid physical machine which minimizes the resulting variance on the number of virtual machines on each physical machine.
- **Reserve:** This algorithm performs a heuristic 1-step planning in the face of uncertainty. It has two modes to model the uncertainty in future VM requests:
 - **Reserve Offline:** Expects a histogram of VM request types (provided via profiled demand during initialization), signifying the expected demand for that VM type over the long-run horizon.

- **Reserve Online:** Agent will maintain a histogram of seen VM requests, and pretends that the histogram at time t is a good-enough summary of demands $[t + 1, T]$.

The agent will attempt to keep PMs in reserve so as to serve a potential future demand for each VM type proportional to its histogram value. The minimum reserved parameter set during initialization specifies how many instances of the most-in-demand VM should be serviceable by the reserve capacity.

When required to allocate a VM request, the agent considers each possible next state when allocating to each valid PM. Then it computes how much capacity that next state would have for every VM type and compares this with the reserves that it must maintain.

This is a custom designed heuristic which achieved good performance. In particular, on the same measurement as Table 1 we saw that Reserve Offline had a measure of -0.45 ± 0.13 and Reserve Online as -0.36 ± 0.14 . However, both algorithms were evaluated on and used the evaluation trace dataset when updating their histogram over the demands for the different VM types. As such, we omitted them from Table 1.

E.6.2 Sim2Real RL Algorithms

We also compared our HINDSIGHT LEARNING approaches to existing Sim2Real RL algorithms in the literature with custom implementation built on top of the MARO package. These include:

- **Deep Q Network (DQN):** Double Q -Learning algorithm from [73].
- **Actor Critic (AC):** Actor Critic algorithm implementation from [48].
- **Mean Actor Critic (MAC):** A modification of the actor critic algorithm where the actor loss is calculated along all actions instead of just the selected actions [6].
- **Policy Gradient (VPG):** A modification of the vanilla policy gradient with a exogenous input dependent baseline from [55]. Instead of training a baseline explicitly, we use $Q_t^{\text{Best Fit}}(s, a, \xi_{\geq t})$.

E.7 State Features, Network Architecture, and Hyperparameters

The state space of the VM allocation scenario is combinatorial as we need to include the CPU and memory utilization of each physical machine across time to account for the lifetimes of the VMs currently assigned to the PM. To rectify this, for each of the deep RL algorithms we use action-dependent features when representing the state space. In particular, once a VM request arrives, we consider the set of physical machines that are available to service this particular virtual machine. Each (PM, VM) pair has associated state features, including:

- The VM’s CPU cores requirement, memory requirement, and lifetime
- The PM’s CPU cores capacity, memory capacity, and type
- The historical CPU cores allocated, utilization, energy consumption, and memory allocated over last three VM requests

The last component is serving as a proxy for the historical utilization of the PM across all time to account for all VMs currently assigned to the PM. The final action dependent features corresponds to the concatenation of these state features for each valid PM to service the current request.

We note that to use action-dependent features some of the algorithms required slight tweaking to their implementations. In particular, when considering algorithms using a policy network representation (i.e. policy gradient, actor critic, or mean actor critic) when executing the policy we take $\pi_\theta = \text{Softmax}(\pi(s, a_1), \dots, \pi(s, a_N))$ where a_1, \dots, a_N is the set of physical machines that can service the current request and (s, a_i) is the corresponding state-features for the physical machine a_i .

For both the actor and critic network representations we use a four layer neural network with (32, 16, 8) hidden dimensions, an output dimension of one (due to the action-dependent features), and LeakyReLU activation functions. For each of the algorithms we use the *RMSprop* optimization algorithm.

Lastly we provide a list of the hyperparameters used and which algorithm they apply to when tuning algorithm performance.

Table 3: List of hyperparameters tuned over for the Sim2Real RL and HINDSIGHT LEARNING algorithms.

Hyperparameter	Algorithm	Values
Discount Factor	DQN, AC, MAC, PG	0.9, 0.95, 0.99, 0.999
Learning Rate	All Algorithms	0.05, 0.005, 0.0005, 0.00005, 0.000005
Entropy Regularization	PG, AC, MAC	0, 0.1, 1, 10
Actor Loss Coefficient	AC, MAC	0.1, 1, 10, 100
Target Update Smoothing Parameter	DQN	0.0001, 0.001, 0.01, 0.1

For concrete parameters evaluated and experiment results, see the attached code-base.

E.8 Training Performance

In Figure 5 we include a plot of the loss curves for the various algorithms.

E.9 Testing Performance

In Table 4 we plot the performance of the algorithms on the true reward function. Here we include the true reward considered:

$$r(s, a, \xi) = -100 * \text{Failed-Allocation} - 1/\text{Packing Density}(s)$$

as well as simply $\text{Packing Density}(s)$. All measures are reported with a 95% confidence interval, and computed as differences against the **Best Fit** allocation policy.

F Omitted Proofs

In this section we include the proofs for all of the results presented in the main paper.

Lemma 9 (Lemma 1 of Main Paper). *For every $t \in [T]$, $(s, a) \in \mathcal{S} \times \mathcal{A}$, and $\pi \in \Pi$, we have the following:*

$$\begin{aligned} Q_t^\pi(s, a) &= \mathbb{E}_{\xi_{\geq t}}[Q_t^\pi(s, a, \xi_{\geq t})] \\ V_t^\pi(s) &= \mathbb{E}_{\xi_{\geq t}}[V_t^\pi(s, \xi_{\geq t})]. \end{aligned}$$

In particular $V_1^\pi(s_1) = V_1^\pi = \mathbb{E}_\xi[V_1^\pi(s_1, \xi)]$.

Table 4: Performance of heuristics, Sim2Real RL, and HINDSIGHT LEARNING algorithms on VM allocation. Here we include the true reward metric the algorithms were trained on (negative inverse of the packing density) and the packing density improvements on average.

Algorithm	Performance $r = -1/\text{Packing Density}$	Packing Density
Performance Upper Bound	0.66 ± 0.29	$.09\% \pm 0.03\%$
Best Fit	0.0	0.0
Bin Packing	-64.44 ± 2.49	$-5.34\% \pm 0.2\%$
Round Robin	-56.36 ± 2.65	$-4.67\% \pm 0.22\%$
Random	-48.94 ± 2.33	$-4.08\% \pm 0.19\%$
DQN	-1.00 ± 0.41	$-0.05\% \pm 0.04\%$
MAC	-0.38 ± 0.033	$-0.03\% \pm 0.00\%$
AC	-2.94 ± 0.61	$-0.21\% \pm 0.06\%$
Policy Gradient	-1.03 ± 0.39	$-0.06\% \pm 0.04\%$
Hindsight MAC	0.18 ± 0.093	$0.05\% \pm 0.00\%$
HINDSIGHT Q-DISTILLATION	0.08 ± 0.32	$0.04\% \pm 0.029\%$

Proof. First note that if $Q_t^\pi(s, a)$ is as defined then we have that:

$$\begin{aligned}
 V_t^\pi(s) &= \sum_a \pi(a | s) Q_t^\pi(s, a) \text{ (by Bellman equations)} \\
 &= \sum_a \pi(a | s) \mathbb{E}_{\xi_{\geq t}} [Q_t^\pi(s, a, \xi_{\geq t})] \\
 &= \mathbb{E}_{\xi_{\geq t}} \left[\sum_a \pi(a | s) Q_t^\pi(s, a, \xi_{\geq t}) \right] \text{ (by } \pi \text{ being non-anticipatory)} \\
 &= \mathbb{E}_{\xi_{\geq t}} [V_t^\pi(s, \xi_{\geq t})].
 \end{aligned}$$

Now we focus on showing the result for $Q_t^\pi(s, a)$ by backwards induction on t . The base case when $t = T$ is trivial as $Q_T^\pi(s, a) = \mathbb{E}_\xi [r(s, a, \xi)] = \mathbb{E}_{\xi_{\geq T}} [Q_T^\pi(s, a, \xi_{\geq T})]$.

Step Case: ($t + 1 \rightarrow t$) For the step-case a simple derivation shows that

$$\begin{aligned}
 Q_t^\pi(s, a) &= \mathbb{E}_\xi [r(s, a, \xi) + V_{t+1}^\pi(f(s, a, \xi))] \\
 &= \mathbb{E}_\xi [r(s, a, \xi) + \mathbb{E}_{\xi_{\geq t+1}} [V_{t+1}^\pi(f(s, a, \xi), \xi_{\geq t+1})]] \\
 &= \mathbb{E}_{\xi_{\geq t}} [r(s, a, \xi_t) + V_{t+1}^\pi(f(s, a, \xi_t), \xi_{\geq t+1})] \\
 &= \mathbb{E}_{\xi_{\geq t}} [Q_t^\pi(s, a, \xi_{\geq t})].
 \end{aligned}$$

□

Lemma 10 (Lemma 2 of Main Paper). *There exists a set of Exo-MDPs such that $\text{REGRET}(\pi^\dagger) \geq \Omega(T)$.*

Proof. We first construct a three-step MDP such that $\text{REGRET}(\pi^\dagger) \geq \Omega(1)$. The main result then follows by replicating the MDP across T periods to construct a $3T$ step MDP with $\text{REGRET}(\pi^\dagger) \geq \Omega(T)$.

We consider a modification of the prototypical Pandora’s Box problem [79]. The endogenous state space $\mathcal{X} = \{0, 1\}$ where state 0 corresponds to “not yet accepted an item” and 1 corresponds

to “accepted an item”. The action space $\mathcal{A} = \{0, 1\}$ where $a = 0$ corresponds to “reject next item” and $a = 1$ corresponds to “accept next item”. We consider a modification of the typical Pandora box model where at time step t , the next item arrivals ξ_t value is unobserved before deciding whether or not to accept.

The trace distribution has $\xi_1 \sim U[0, 1]$ and $\xi_2, \xi_3 \sim U[0, .9]$. Important to note is that $\mathbb{E}[\xi_1] = .5, \mathbb{E}[\xi_2] = 0.45, \mathbb{E}[\xi_3] = 0.45$, and a straightforward calculation shows that $\mathbb{E}[\max(\xi_2, \xi_3)] = 0.6$.

The rewards and dynamics are:

$$\begin{aligned} r(0, 0, \xi) &= 0 & f(0, 0, \xi) &= 0 \\ r(0, 1, \xi) &= \xi & f(0, 1, \xi) &= 1 \\ r(1, \cdot, \xi) &= 0 & f(1, a, \xi) &= 1 \text{ for } a \in \{0, 1\}. \end{aligned}$$

Lastly, the starting state $s_1 = 0$. This properly encodes the exogenous dynamics and rewards. At step t in state $x = 0$ (i.e. not yet accepted an item) taking action 0 (do not accept) yields no return and transitions to the next state. However, accepting the next item returns reward ξ and transitions to state $x = 1$.

A straightforward calculation following the Bellman equations shows the following for Q_t^* and V_t^* :

$$\begin{aligned} Q_3^*(0, 0) &= 0 & Q_2^*(0, 0) &= \mathbb{E}[\xi_3] & Q_1^*(0, 0) &= \max(\mathbb{E}[\xi_2], \mathbb{E}[\xi_3]). \\ Q_3^*(0, 1) &= \mathbb{E}[\xi_3] & Q_2^*(0, 1) &= \mathbb{E}[\xi_2] & Q_1^*(0, 1) &= \mathbb{E}[\xi_1] \\ Q_3^*(1, \cdot) &= 0 & Q_2^*(1, \cdot) &= 0 & Q_1^*(1, \cdot) &= 0 \\ V_3^*(0) &= \mathbb{E}[\xi_3] & V_2^*(0) &= \max(\mathbb{E}[\xi_3], \mathbb{E}[\xi_2]) & V_1^*(0) &= \max(\mathbb{E}[\xi_1], \mathbb{E}[\xi_2], \mathbb{E}[\xi_3]) \\ V_3^*(1) &= 0 & V_2^*(1) &= 0 & V_1^*(1) &= 0. \end{aligned}$$

Using the choice of the distributions for ξ_1, ξ_2, ξ_3 we have that $\pi_1^*(0) = 1$, as in, we will accept the first item since on average it has larger expected return. This results in $V_1^{\pi^*}(s_1) = \mathbb{E}[\xi_1] = 0.5$.

We can similarly compute Q_t^\dagger and V_t^\dagger as follows:

$$\begin{aligned} Q_3^\dagger(0, 0) &= 0 & Q_2^\dagger(0, 0) &= \mathbb{E}[\xi_3] & Q_1^\dagger(0, 0) &= \mathbb{E}[\max(\xi_2, \xi_3)]. \\ Q_3^\dagger(0, 1) &= \mathbb{E}[\xi_3] & Q_2^\dagger(0, 1) &= \mathbb{E}[\xi_2] & Q_1^\dagger(0, 1) &= \mathbb{E}[\xi_1] \\ Q_3^\dagger(1, \cdot) &= 0 & Q_2^\dagger(1, \cdot) &= 0 & Q_1^\dagger(1, \cdot) &= 0. \end{aligned}$$

In this scenario, we see first hand the bias introduced when considered Q^\dagger . In particular, $Q_1^\dagger(0, 0) = \mathbb{E}[\max(\xi_2, \xi_3)] \geq Q_1^*(0, 0) = \max(\mathbb{E}[\xi_2, \xi_3])$. Using the choice of distributions for ξ_1, ξ_2, ξ_3 we see that the hindsight planning policy π^\dagger is fooled and has $\pi_1^\dagger(0) = 0$, so the policy rejects the first item thinking it will get the maximum value of the next two items. As a result we see that $V_1^{\pi^\dagger}(0) = 0.45$.

Hence, we have that $\text{REGRET}^{\pi^\dagger} = 0.5 - 0.45 = 0.05 = \Omega(1)$ as needed. \square

This example highlights that HINDSIGHT LEARNING is not for *every* Exo-MDP. To leverage the hindsight planning policy for general Exo-MDPs, the bias needs to be properly controlled.

Lemma 11 (Lemma 3 of Main Paper). $\text{REGRET}(\pi^\dagger) \leq \sum_{t=1}^T \mathbb{E}_{S_t \sim \text{Pr}_t^{\pi^\dagger}} [\Delta_t^\dagger(S_t)]$ where $\text{Pr}_t^{\pi^\dagger}$ denotes the state distribution of π^\dagger at step t induced by the exogenous randomness. In particular, if $\Delta_t^\dagger(s) \leq \Delta$ for some constant Δ then we have: $\text{REGRET}(\pi^\dagger) \leq \Delta \sum_{t=1}^T \mathbb{E}_{S_t \sim \text{Pr}_t^{\pi^\dagger}} [\text{Pr}(\pi_t^\dagger(S_t) \neq \pi^*(S_t))]$.

Proof. First we note that via the performance difference lemma we have that for any two non-anticipatory policies π and $\tilde{\pi}$ that

$$\begin{aligned} V_1^\pi(s_1) - V_1^{\tilde{\pi}}(s_1) &= \sum_{t=0}^{T-1} \mathbb{E}_{s_t \sim \text{Pr}_t^{\tilde{\pi}}} \left[\sum_a \pi(a | s_t) (Q_h^{\tilde{\pi}}(s, a) - V_h^{\tilde{\pi}}(s)) \right] \text{ and so} \\ V_1^{\tilde{\pi}}(s_1) - V_1^\pi(s_1) &= \sum_{t=0}^{T-1} \mathbb{E}_{s_t \sim \text{Pr}_t^\pi} \left[\sum_a \pi(a | s_t) (V_h^{\tilde{\pi}}(s) - Q_h^{\tilde{\pi}}(s, a)) \right] \end{aligned}$$

Moreover, for any state s we also have $Q_t^*(s, \pi^*(s)) - Q_t^*(s, \pi^\dagger(s)) \leq \Delta_t^\dagger(s)$ since:

$$\begin{aligned} &Q_t^*(s, \pi^*(s)) - Q_t^*(s, \pi^\dagger(s)) - \Delta_t^\dagger(s) \\ &= Q_t^*(s, \pi^*(s)) - Q_t^*(s, \pi^\dagger(s)) - Q_t^\dagger(s, \pi^\dagger(s)) + Q_t^*(s, \pi^\dagger(s)) - Q_t^*(s, \pi^*(s)) + Q_t^\dagger(s, \pi^*(s)) \\ &= Q_t^\dagger(s, \pi^*(s)) - Q_t^\dagger(s, \pi^\dagger(s)) \leq 0 \end{aligned}$$

as π^\dagger is greedy with respect to Q^\dagger .

Finally, recall the definition of the regret of $\text{REGRET}(\pi^\dagger)$ via $V_1^*(s_1) - V_1^{\pi^\dagger}(s_1)$. However, using the previous performance difference lemma with $\tilde{\pi} = \pi^*$ and $\pi = \pi^\dagger$ we have that

$$\begin{aligned} V_1^*(s_1) - V_1^{\pi^\dagger}(s_1) &= \sum_t \mathbb{E}_{S_t \sim \text{Pr}_t^{\pi^\dagger}} \left[Q_t^*(S_t, \pi^*(S_t)) - Q_t^*(S_t, \pi^\dagger(S_t)) \right] \\ &\leq \sum_t \mathbb{E}_{S_t \sim \text{Pr}_t^{\pi^\dagger}} \left[\Delta_t^\dagger(S_t) \right]. \end{aligned}$$

The second statement follows immediately from the absolute bound on $\Delta_t^\dagger(s)$. \square

Theorem 12 (Theorem 4 of Main Paper). *In stochastic online bin packing with i.i.d. arrivals we have that $\sup_{t,s} \Delta_t^\dagger(s) \leq O(1)$, independent of the time horizon and any problem primitives. As a result, $\text{REGRET}(\pi^\dagger) \leq O(1)$.*

We show the result by starting with the lemma, highlighting that the value functions for the planning policy and the optimal non-anticipatory policy are ‘‘Lipschitz’’ with respect to the capacity of the current bins. Recall that the state space representation $s \in \mathcal{S}$ corresponds to $s = (x, \xi_{t-1})$ where $x \in \mathbb{R}^B$ is the current number of bins at that size, and the last component to the current arrival. We write this explicitly as containing $s \in \mathbb{R}^B$ for the bin utilization and $\xi_{t-1} \in \mathbb{R}$ for the current arrival.

Lemma 13. *For any $t \in [T]$, current bin capacity $x \in \mathbb{R}^{|B|}$, current arrival ξ_{t-1} , $\boldsymbol{\xi}_{\geq t} \in \Xi^{T-t}$, and $\Delta \in \mathbb{R}^B \geq 0$ we have that:*

- $V_t^\dagger(x, \xi_{t-1}, \boldsymbol{\xi}_{\geq t}) \geq V_t^\dagger(x - \Delta, \xi_{t-1}, \boldsymbol{\xi}_{\geq t}) \geq V_t^\dagger(x, \xi_{t-1}, \boldsymbol{\xi}_{\geq t}) - \|\Delta\|_1$
- $V_t^*(x, \xi_{t-1}) \geq V_t^*(x - \Delta, \xi_{t-1}) \geq V_t^*(x, \xi_{t-1}) - \|\Delta\|_1$

As a result for any x and x' in \mathbb{R}^B and current arrival ξ_{t-1} we have that:

- $V_t^\dagger(x, \xi_{t-1}, \boldsymbol{\xi}_{\geq t}) - V_t^\dagger(x', \xi_{t-1}, \boldsymbol{\xi}_{\geq t}) \leq \|(x - x')^+\|_1$
- $V_t^*(x, \xi_{t-1}) - V_t^*(x', \xi_{t-1}) \leq \|(x - x')^+\|_1$

Proof. First consider the top statement in terms of the optimal planning policy starting from a fixed state $s = (x, \xi_{t-1})$ and sequence of future exogenous variables $\xi_{\geq t}$.

We have that $V_t^\dagger(x, \xi_{t-1}, \xi_{\geq t}) \geq V_t^\dagger(x - \Delta, \xi_{t-1}, \xi_{\geq t})$ since the sequence of actions generated by the planning oracle starting from state $(x - \Delta, \xi_{t-1})$ is feasible for the same problem starting from (x, ξ_{t-1}) . Hence, as $V_t^\dagger(x, \xi_{t-1}, \xi_{\geq t})$ denotes the optimal such policy, the inequality follows.

For the other direction consider the sequence of actions starting from (x, ξ_{t-1}) . Using at most $\|\Delta\|_1$ bins the policy is feasible for the same problem starting at $(x - \Delta, \xi_{t-1})$. Indeed, suppose the sequence of actions starting from the problem at (x, ξ_{t-1}) attempts to use a bin which is not available in the problem starting from $(x - \Delta, \xi_{t-1})$. Then by opening a new bin instead and shifting all future references of the old bin to the newly created bin, the sequence of actions is feasible. As there are at most $\|\Delta\|_1$ bins different in the (x, ξ_{t-1}) problem versus the $(x - \Delta, \xi_{t-1})$ problem, the bound follows.

Now consider the second statement in terms of the optimal non-anticipatory policy starting from a fixed state (x, ξ_{t-1}) . First note that $V_t^*(x, \xi_{t-1}) = \mathbb{E}_{\xi_{\geq t}}[V_t^*(x, \xi_{t-1}, \xi_{\geq t})]$ and similarly for $V_t^*(x - \Delta, \xi_{t-1})$. We have that $V_t^*(x, \xi_{t-1}) \geq V_t^*(x - \Delta, \xi_{t-1})$ as the optimal policy starting from $(x - \Delta, \xi_{t-1})$ is feasible on all sample paths generated by $\xi_{\geq t}$ to the same problem starting at (x, ξ_{t-1}) . Hence by optimality of π^* the inequality must follow.

For the other direction, on any sample path consider the sequence of actions generated by the optimal policy starting from (x, ξ_{t-1}) . By a similar argument, again using at most $\|\Delta\|_1$ extra bins the policy is feasible for the problem starting at $(x - \Delta, \xi_{t-1})$. Hence by optimality, the inequality follows.

The second result follows via straightforward algebraic manipulations. Indeed, the previous statement can be thought of as showing that for $x \in \mathbb{R}^B$ and $\Delta \in \mathbb{R}_+^B$ that $f(x) \geq f(x - \Delta) \geq f(x) - \|\Delta\|_1$. However,

$$f(x) - f(x') = f(x) - f(x' + (x - x')^+) + f(x' + (x - x')^+) - f(x') \leq f(x' + (x - x')^+) - f(x') \leq \|(x - x')^+\|_1$$

where the first inequality uses that $x' + (x - x')^+ \geq x$ and the second the previous result. \square

We are now ready to show the bound that $\Delta_t^\dagger(s) \leq O(1)$.

Proof. For a fixed time t and state s consider $\Delta_t^\dagger(s) = Q_t^\dagger(s, \pi^\dagger(s)) - Q_t^*(s, \pi^\dagger(s)) + Q_t^*(s, \pi^*(s)) - Q_t^\dagger(s, \pi^*(s))$

However consider $Q_t^\dagger(s, \pi^\dagger(s)) - Q_t^\dagger(s, \pi^*(s))$ (with the other term dealt with similarly). On any sample path, the difference in these terms is bounded by the immediate reward plus the difference of the value at the next states. By problem definition, the difference in immediate rewards is bounded by one. However, consider the difference in value functions at the next state. Their state representation has a value of $\|(x - x')^+\|_1$ of at most 2 (for the two bins that were potentially modified). Hence, this difference is bounded by 3 in total. A similar argument for Q^* completes the proof. \square

Lemma 14 (Statement in Section 4). *Suppose that for every t and state s that $\max_{\pi \in \Pi} \mathbb{E}_{\xi_{\geq t}}[V_t^\pi(s, \xi_{\geq t})] = \mathbb{E}_{\xi_{\geq t}}[\text{HINDSIGHT}(t, s, \xi_{\geq t})]$. Then we have that $Q_t^*(s, a) = Q_t^\dagger(s, a)$ for every t, s , and a .*

Proof. First notice that $\max_{\pi \in \Pi} \mathbb{E}_{\xi_{\geq t}}[V_t^\pi(s, \xi_{\geq t})] = \mathbb{E}_{\xi_{\geq t}}[V_t^*(s, \xi_{\geq t})]$ by definition. Thus using the Bellman equations and definition of $Q_t^\dagger(s, a)$ we trivially have that:

$$\begin{aligned} Q_t^*(s, a) &= \mathbb{E}_{\xi_t}[r(s, a, \xi_t) + V_{t+1}^*(f(s, a, \xi_t))] \\ &= \mathbb{E}_{\xi_t}[r(s, a, \xi_t) + \mathbb{E}_{\xi_{>t}}[V_{t+1}^*(f(s, a, \xi_t), \xi_{>t})]] \end{aligned}$$

$$\begin{aligned}
&= \mathbb{E}_{\xi_t}[r(s, a, \xi_t) + \mathbb{E}_{\xi_{>t}}[\text{HINDSIGHT}(t+1, f(s, a, \xi_t), \xi_{>t})]] \\
&= Q_t^\dagger(s, a).
\end{aligned}$$

□

Theorem 15 (Theorem 5 of the main paper). *Let $\bar{\pi}^\dagger$ denote the hindsight planning surrogate policy for the empirical MDP w.r.t. \mathcal{D} . Assume $\bar{\pi}^\dagger \in \Pi$ and Algorithm 1 achieves no-regret in the optimization problem. Let π be the best policy generated by Algorithm 1. Then, for any $\delta \in (0, 1)$, with probability $1 - \delta$, it holds*

$$\text{REGRET}(\pi) \leq T \sqrt{\frac{2 \log(2|\Pi|/\delta)}{N}} + \sum_{t=1}^T \mathbb{E}_{s_t \sim \bar{P}_t^{\bar{\pi}^\dagger}} [\bar{\Delta}_t^\dagger(s_t)] + o(1)$$

where $\bar{\Delta}_t^\dagger$ is the SAA approximation of (9) and $\bar{P}_t^{\bar{\pi}^\dagger}$ is the state probability of $\bar{\pi}^\dagger$ in the empirical MDP.

Proof. The proof follows the standard proof technique of online IL (cf. [81]).

$$\begin{aligned}
\text{REGRET}(\pi) &= \mathbb{E}[V_1^*(s_1, \boldsymbol{\xi})] - \mathbb{E}[V_1^\pi(s_1, \boldsymbol{\xi})] \\
&\leq \left(|\mathbb{E}[V_1^\pi(s_1, \boldsymbol{\xi})] - \mathbb{E}[V_1^{\pi^*}(s_1, \boldsymbol{\xi})]| + |\mathbb{E}[V_1^{\pi^*}(s_1, \boldsymbol{\xi})] - \mathbb{E}[V_1^{\bar{\pi}^\dagger}(s_1, \boldsymbol{\xi})]| \right) \\
&\quad + \left(\mathbb{E}[V_1^{\pi^*}(s_1, \boldsymbol{\xi})] - \mathbb{E}[V_1^{\bar{\pi}^\dagger}(s_1, \boldsymbol{\xi})] + \mathbb{E}[V_1^{\bar{\pi}^\dagger}(s_1, \boldsymbol{\xi})] - \mathbb{E}[V_1^\pi(s_1, \boldsymbol{\xi})] \right) \\
&\leq 2T \sqrt{\frac{2 \log(2|\Pi|/\delta)}{N}} + \mathbb{E}[V_1^{\pi^*}(s_1, \boldsymbol{\xi})] - \mathbb{E}[V_1^{\bar{\pi}^\dagger}(s_1, \boldsymbol{\xi})] + o(1) \\
&\leq 2T \sqrt{\frac{2 \log(2|\Pi|/\delta)}{N}} + \sum_{t=1}^T \mathbb{E}_{s_t \sim \bar{P}_t^{\bar{\pi}^\dagger}} [\bar{\Delta}_t^\dagger(s_t)] + o(1)
\end{aligned}$$

We use the results of Theorem 17 to bound the first terms in the second line; we invoke the no-regret optimization assumption and the realizability assumption $\bar{\pi}^\dagger \in \Pi$ for the last term of the second line. Finally, we apply Lemma 3 in the empirical MDP w.r.t. \mathcal{D} and recognize that the middle term is the empirical regret to derive the last step. □

Theorem 16 (Theorem 6 of Main Paper). *Suppose that $\sup_{t \in [T], \xi_{<t} \in \Xi^{[t-1]}} \|\bar{\mathcal{P}}_\Xi(\cdot | \xi_{<t}) - \mathcal{P}_\Xi(\cdot | \xi_{<t})\|_{TV} \leq \epsilon$ where $\|\cdot\|_{TV}$ is the total variation distance. Then we have that $\text{REGRET}(\bar{\pi}) \leq 2T^2 \epsilon$. In addition, if $\boldsymbol{\xi} \sim \mathcal{P}_\Xi$ has each ξ_t independent from $\xi_{<t}$, $\bar{\mathcal{P}}_\Xi$ is the empirical distribution, then $\forall \delta \in (0, 1)$, with probability at least $1 - \delta$, $\text{REGRET}(\bar{\pi}) \leq 2T^2 \sqrt{\frac{\log(2|\Xi|/\delta)}{N}}$.*

Proof. First note that \bar{Q}_t and \bar{V}_t refer to the Q and V values for the optimal policy in a modified MDP \bar{M} where the true exogenous input distribution $\mathcal{P}_\Xi(\cdot | \xi_{<t})$ is replaced by its estimate $\bar{\mathcal{P}}_\Xi(\cdot | \xi_{<t})$. As such, denote by \bar{V}_t^π as the value function for the policy π in the MDP \bar{M} . Note here that $\bar{V}_t^\pi = \bar{V}_t$ by construction. With this we have that:

$$\begin{aligned}
\text{REGRET}(\bar{\pi}) &= V_1^*(s_1) - V_1^{\bar{\pi}}(s_1) \\
&= V_1^*(s_1) - \bar{V}_1^{\pi^*}(s_1) + \bar{V}_1^{\pi^*}(s_1) - \bar{V}_1(s_1) + \bar{V}_1(s_1) - V_1^{\bar{\pi}}(s_1) \\
&\leq 2 \sup_{\pi} |V_1^\pi(s_1) - \bar{V}_1^\pi(s_1)|.
\end{aligned}$$

However, using the finite horizon simulation lemma (see Lemma 1 in [1]) we have that this is bounded from above by $2T^2\|p(\cdot | s, a) - \bar{p}(\cdot | s, a)\|_{TV}$ where $\|p(\cdot | s, a) - \bar{p}(\cdot | s, a)\|_{TV}$ is the total variation distance in the induced state-transition distributions between M and \bar{M} . However, by definition we have that:

$$\begin{aligned}\|p(\cdot | s, a) - \bar{p}(\cdot | s, a)\|_{TV} &= \frac{1}{2} \int_{\mathcal{S}} |p(s' | s, a) - \bar{p}(s' | s, a)| ds \\ &= \frac{1}{2} \int_{\mathcal{S}} \left| \int_{\Xi} \mathbb{1}_{[s'=f(s,a,\xi)]} d\mathcal{P}_{\Xi}(\xi | \xi_{\geq t}) - \int_{\Xi} \mathbb{1}_{[s'=f(s,a,\xi)]} d\bar{\mathcal{P}}_{\Xi}(\xi | \xi_{\geq t}) \right| ds \\ &= \frac{1}{2} \int_{\mathcal{S}} \left| \int_{\Xi} \mathbb{1}_{[s'=f(s,a,\xi)]} |d\mathcal{P}_{\Xi}(\xi | \xi_{\geq t}) - d\bar{\mathcal{P}}_{\Xi}(\xi | \xi_{\geq t})| \right| \\ &\leq \|\mathcal{P}_{\Xi}(\cdot | \xi_{\geq t}) - \bar{\mathcal{P}}_{\Xi}(\cdot | \xi_{\geq t})\|_{TV} \leq \epsilon.\end{aligned}$$

Thus we get that $\text{REGRET}(\bar{\pi}) \leq 2T^2\epsilon$ as required.

Now suppose that $\xi \sim \mathcal{P}_{\Xi}$ has each ξ_t independent from $\xi_{<t}$ and let $\bar{\mathcal{P}}_{\Xi}$ be the empirical distribution, i.e. $\bar{\mathcal{P}}_{\Xi}(\xi) = \frac{1}{N} \sum_{i \in [N]} \mathbb{1}_{[\xi_i = \xi]}$. A straightforward application of Hoeffding's inequality shows that the event:

$$\mathcal{E} = \left\{ \forall t, \xi_{<t} : |\bar{\mathcal{P}}_{\Xi}(\Xi) - \mathcal{P}_{\Xi}(\xi)| \leq \sqrt{\frac{\log(2|\Xi|/\delta)}{2N}} \right\}$$

occurs with probability at least $1 - \delta$. Under \mathcal{E} we then have that:

$$\sup_{t \in [T], \xi_{<t} \in \Xi^{[t-1]}} \|\bar{\mathcal{P}}_{\Xi}(\cdot | \xi_{<t}) - \mathcal{P}_{\Xi}(\cdot | \xi_{<t})\|_{TV} \leq \sup_{t \in [T], \xi_{<t} \in \Xi^{[t-1]}} \|\bar{\mathcal{P}}_{\Xi}(\cdot | \xi_{<t}) - \mathcal{P}_{\Xi}(\cdot | \xi_{<t})\|_1 \leq \sqrt{\frac{\log(2|\Xi|/\delta)}{2N}}.$$

Taking this in the previous result shows the claim. \square

Theorem 17 (Theorem 7 of Main Paper). *Given any $\delta \in (0, 1)$ then with probability at least $1 - \delta$ we have that if $\bar{\pi}^* = \text{argmax}_{\pi} \bar{\mathbb{E}}[V^{\pi}(\xi)]$ that*

$$\text{REGRET}(\bar{\pi}^*) \leq \sqrt{\frac{2T^2 \log(2|\Pi|/\delta)}{N}}.$$

Proof. A quick calculation using Hoeffding's inequality and a union bound shows that the event

$$\mathcal{E} = \left\{ \forall \pi \in \Pi : |V_1^{\pi}(s_1) - \bar{\mathbb{E}}[V_1^{\pi}(s_1)]| \leq \sqrt{\frac{T^2 \log(2|\Pi|/\delta)}{2N^2}} \right\}$$

occurs with probability at least $1 - \delta$. Under \mathcal{E} we then have that:

$$\begin{aligned}\text{REGRET}(\bar{\pi}^*) &= V_1^{\bar{\pi}^*}(s_1) - V_1^{\bar{\pi}^*}(s_1) \\ &= V_1^{\bar{\pi}^*}(s_1) - \bar{\mathbb{E}}[V_1^{\bar{\pi}^*}(s_1, \xi)] + \bar{\mathbb{E}}[V_1^{\bar{\pi}^*}(s_1, \xi)] - \bar{\mathbb{E}}[V_1^{\bar{\pi}^*}(s_1, \xi)] + \bar{\mathbb{E}}[V_1^{\bar{\pi}^*}(s_1, \xi)] - V_1^{\bar{\pi}^*}(s_1) \\ &\leq 2\sqrt{\frac{V_{max}^2 \log(2|\Pi|/\delta)}{2N^2}}.\end{aligned}$$

\square

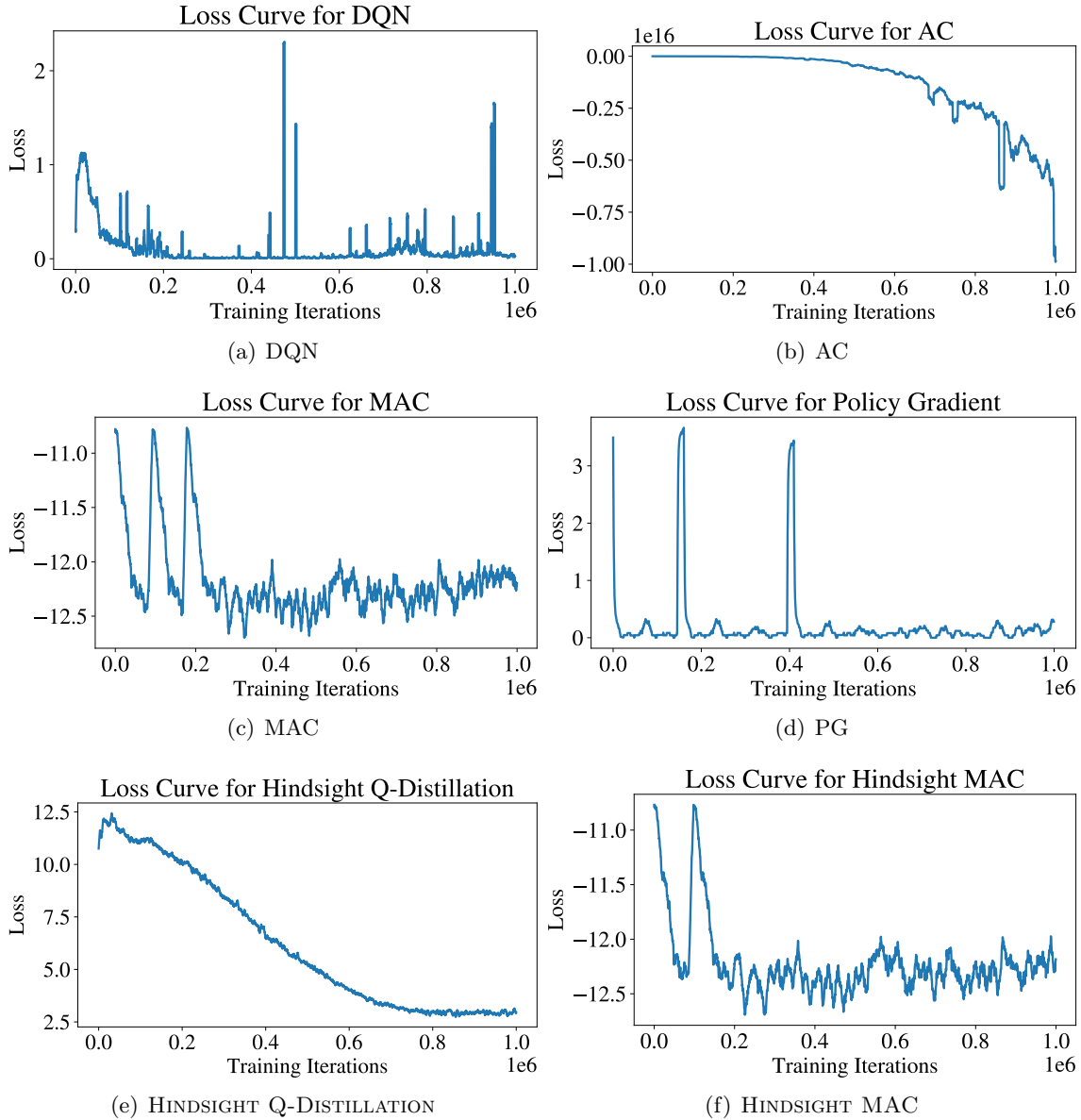


Figure 5: Moving average of the loss curves for the Sim2Real RL and HINDSIGHT LEARNING algorithms over the one million gradient steps computed in each of the experiments. Note that some of the volatility occurs when an algorithm observes a datapoint with a failed allocation as there is a large penalty.